Interfacial Micromechanics Assessment of Classical Rheological Models. II: Multiple Interface Sizes and Viscosities

M. Shahidi[1]; B. Pichler, Aff.M.ASCE[2]; and Ch. Hellmich, M.ASCE[3]

Abstract: Whereas the companion paper provided a micromechanical explanation of the spring and dashpot parameters occurring in the rheological models of the Kelvin-Voigt and Maxwell type, we here extend this discussion toward rheological chain models. Therefore, the considered micromechanical system is extended from one interface phase to N interface phases differing in size and viscosity. Elimination schemes allow for deriving differential equations with only overall stresses and strains and their derivatives as unknowns, rather than microstresses and microstrains in case of micromechanics, or spring/dashpot-related stresses and strains in case of the rheological chain models. Comparison of corresponding coefficients reveals a full analogy between the two different types of chain models, and also between the latter and the micromechanics model. For the Kelvin-Voigt chain, this analogy is even identical to the one of the Zener model of companion paper Part I. The Maxwell chain-related analogy is much more complex, and analytical solutions only exist in the case of very few chain units. **DOI: 10.1061/(ASCE)EM.1943-7889.0001013.**

Author keywords: Kelvin-Voigt model; Maxwell model; Chain models; Viscoelasticity; Creep; Relaxation.

Introduction

Whereas the rheological models of the Maxwell and the Kelvin-Voigt type, which combine, in different ways, two springs and one dashpot, are often helpful to illustrate principal features of the creep and relaxation characteristics of various materials, they often appear as too simple when it comes to the representation of the actual material behavior. This was realized already in the 19th century when the field of creep mechanics was initiated (Meyer 1878), and the problem was tackled by the introduction of rheological chain models, such as (1) Maxwell chains, representing a parallel arrangement of several Maxwell units (Maxwell 1867) and an additional spring, and (2) Kelvin-Voigt chains, representing a serial arrangement of several Kelvin-Voigt units (Thomson 1865; Voigt 1890) and an additional spring. Ever since, these models and/or combinations of them have enjoyed great popularity in a variety of applications, concerning, e.g., the creep of non-aging (Šmilauer and Bažant 2010) and aging cementitious materials (Bažant 1977; Bažant et al. 1997; Bažant and Xi 1995), of soft biomaterials such as intervertebral discs (Kelley et al. 1983), or of different types of polymers and plastics (Liu et al. 2008). Extending the discussion developed in the companion paper (Shahidi et al. 2015b), we here ask the question whether also the aforementioned chain models can be directly related to the mechanics of microstructural systems consisting of an elastic solid matrix and viscous interfaces embedded therein. Thereby, as in the companion paper, Part I (Shahidi et al. 2015b), we consider the somehow most reduced and simplest system, which consists of 2D planar "idealized" interfaces—however, now exhibiting different sizes and viscosities. In more detail, we compare (1) coefficients of macroscopic stress-strain relations of rheological chains models with N Kelvin-Voigt units (or N Maxwell units, respectively) with (2) coefficients of stress-strain relations characterizing a matrix-interface composite consisting of a contiguous, isotropic, and linear elastic solid matrix, as well as of N families of parallel interfaces. By analogy to the companion paper (Shahidi et al. 2015b), our focus lies on time-dependent behavior under pure shear. Given interfaces with normals pointing in $\underline{e}_z$ direction, the composite is susceptible to time-dependent behavior when subjected to shear in the x, z-plane and/or in the y, z-plane. Without loss of generality, we here focus on the former case, i.e., we study the relation between macroscopic stresses

$$\underline{\underline{\Sigma}} = \Sigma_{xz}(\underline{e}_x \otimes \underline{e}_z + \underline{e}_z \otimes \underline{e}_x) \tag{1}$$

and strains

$$\underline{\underline{E}} = E_{xz}(\underline{e}_x \otimes \underline{e}_z + \underline{e}_z \otimes \underline{e}_x) \tag{2}$$

As for the structure of this paper, we devote the two following sections to rheological chain models (of the Kelvin-Voigt and the Maxwell type, respectively), and to matrix-interface composites, respectively. In each of these sections, we use specific mathematical schemes for the derivation of stress-strain relations which link shear stresses and their time derivatives to shear strains and their time derivatives. We start with two rheological units or two interface families, respectively, before we then extend the derivation to three rheological units or three interface families, respectively. Finally, we tackle the case of N rheological units or N interface families,

[1]Research Assistant, Institute for Mechanics of Materials and Structures, TU Wien-Vienna Univ. of Technology, Karlsplatz 13/202, A-1040 Vienna, Austria. E-mail: Mehran.Shahidi@boku.ac.at

[2]Associate Professor, Institute for Mechanics of Materials and Structures, TU Wien-Vienna Univ. of Technology, Karlsplatz 13/202, A-1040 Vienna, Austria. E-mail: Bernhard.Pichler@tuwien.ac.at

[3]Full Professor, Institute for Mechanics of Materials and Structures, TU Wien-Vienna Univ. of Technology, Karlsplatz 13/202, A-1040 Vienna, Austria (corresponding author). E-mail: Christian.Hellmich@tuwien.ac.at

Note. This manuscript was submitted on December 24, 2014; approved on August 11, 2015; published online on October 13, 2015. Discussion period open until March 13, 2016; separate discussions must be submitted for individual papers. This paper is part of the ***Journal of Engineering Mechanics***, © ASCE, ISSN 0733-9399.

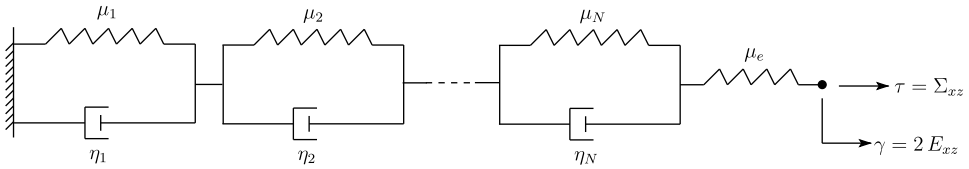

Fig. 1. Kelvin-Voigt chain, used to model time-dependent behavior under pure shear; see Eqs. (1) and (2), with $\Sigma_{xz} = \tau$ and $2E_{xz} = \gamma$

respectively. Therefore, we compare the $2N + 1$ independent coefficients occurring in the constitutive equations derived for the Kelvin-Voigt chain models, the Maxwell chain models, and the micromechanics models with different viscous interface families, respectively. This allows for a micromechanical interpretation of Kelvin-Voigt chain models and Maxwell chain models. The paper closes with a discussion of the results and conclusions.

Review of Rheological Chain Models: Derivation of Governing Differential Equations

Kelvin-Voigt Chain Models

Kelvin-Voigt chain models consist of N Kelvin-Voigt units in series with an additional elastic spring (Fig. 1). The overall shear deformation of the rheological model, $\gamma = 2E_{xz}$ according to Eq. (2), can be decomposed additively into the contributions of the individual Kelvin-Voigt units $(\gamma_1, \gamma_2, \ldots, \gamma_N)$ and into the one of the elastic spring (γ_e)

$$\gamma = \gamma_e + \sum_{i=1}^{N} \gamma_i \tag{3}$$

The overall shear stress $\tau = \Sigma_{xz}$ according to Eq. (1), in turn, is transferred through all N Kelvin-Voigt units $(\tau_1 = \tau_2 = \cdots = \tau_N = \tau)$ and through the elastic spring $(\tau_e = \tau)$, such that

$$\tau = \tau_1 = \tau_2 = \cdots = \tau_N = \tau_e \tag{4}$$

The shear stress acting on the ith Kelvin-Voigt unit can be decomposed into the shear stress acting on the spring, τ_i^{μ}, and into the shear stress acting on the dashpot, τ_i^{η}

$$\tau = \tau_i^{\mu} + \tau_i^{\eta} \quad i = 1,2,\ldots,N \tag{5}$$

where indexes μ and η refer to the spring and to the dashpot, respectively.

The derivation of a constitutive relation between shear stress $\tau = \Sigma_{xz}$ and shear strain $\gamma = 2E_{xz}$, see Eqs. (1) and (2) and Fig. 1, requires individual constitutive laws for all involved rheological devices. Denoting the stiffness of the additional elastic spring as μ_e, the stiffnesses of the Kelvin-Voigt springs as $\mu_1, \mu_2, \ldots, \mu_N$, and the dashpot viscosities as $\eta_1, \eta_2, \ldots, \eta_N$, see Fig. 1, the individual constitutive laws read as

$$\left.\begin{aligned} \tau_i^{\mu} &= \mu_i \gamma_i \\ \tau_i^{\eta} &= \eta_i \dot{\gamma}_i \end{aligned}\right\} \quad i = 1,2,\ldots,N \quad \tau_e = \mu_e \gamma_e \tag{6}$$

where a dot stands for a time derivative

$$\dot{\gamma}_i = \frac{\partial \gamma_i}{\partial t} \tag{7}$$

The sought constitutive relation between τ and γ is obtained by constructing linear combinations between Eqs. (3)–(6) and their time derivatives, yielding, for a chain model with one Kelvin-Voigt unit $(N = 1)$ (Shahidi et al. 2015b)

$$\tau\left(\frac{1}{\mu_e} + \frac{1}{\mu_1}\right) + \dot{\tau}\frac{\eta_1}{\mu_1}\left(\frac{1}{\mu_e}\right) = \gamma + \frac{\eta_1}{\mu_1}\dot{\gamma} \tag{8}$$

In agreement with our current focus on more than one interface size and/or viscosity, we continue with the derivation of the constitutive τ, γ-relation for a chain model with two Kelvin-Voigt units $(N = 2)$, (Fig. 2). In this context, it is beneficial to derive elementary stress-strain relations for the individual Kelvin-Voigt units by specifying Eqs. (5) for the spring and dashpot laws, see Eq. (6), and dividing the resulting expressions by the shear stiffness of the involved spring, yielding

$$\frac{\tau}{\mu_1} = \frac{\eta_1}{\mu_1}\dot{\gamma}_1 + \gamma_1 \tag{9}$$

$$\frac{\tau}{\mu_2} = \frac{\eta_2}{\mu_2}\dot{\gamma}_2 + \gamma_2 \tag{10}$$

By analogy, the shear stress τ_e appearing in the spring law of the additional spring, see Eq. (6), can be set equal to τ, see Eq. (4), and the resulting expression can be solved for γ_e, in order to deliver

$$\frac{\tau}{\mu_e} = \gamma_e \tag{11}$$

Summing up Eqs. (9)–(11) and considering Eq. (3), allow for elimination of γ_1, γ_2, and γ_e

$$\tau\left(\frac{1}{\mu_e} + \frac{1}{\mu_1} + \frac{1}{\mu_2}\right) = \frac{\eta_1}{\mu_1}\dot{\gamma}_1 + \frac{\eta_2}{\mu_2}\dot{\gamma}_2 + \gamma \tag{12}$$

The next step consists of eliminating, from Eq. (12), the first-order derivatives $\dot{\gamma}_1$ and $\dot{\gamma}_2$. Therefore, the first-order time derivatives of Eqs. (9), (10), and (11) are multiplied with η_2/μ_2, with η_1/μ_1, and with $\eta_1/\mu_1 + \eta_2/\mu_2$, respectively, yielding

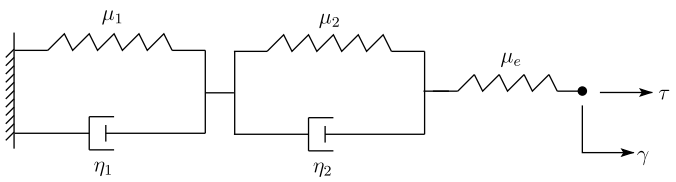

Fig. 2. Kelvin-Voigt chain with two units $(N = 2)$; see Eq. (18) for the governing differential equation

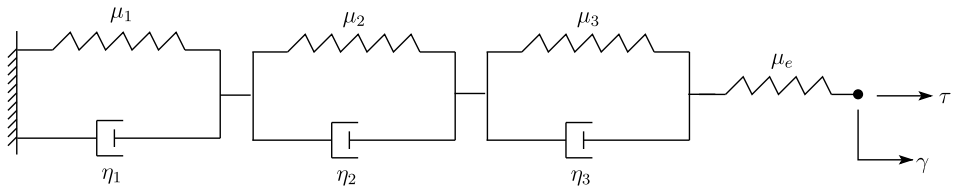

Fig. 3. Kelvin-Voigt chain with three units ($N = 3$); see Eq. (19) for the governing differential equation

$$\frac{\dot{\tau}\eta_2}{\mu_1\mu_2} = \frac{\eta_1}{\mu_1}\frac{\eta_2}{\mu_2}\ddot{\gamma}_1 + \frac{\eta_2}{\mu_2}\dot{\gamma}_1 \tag{13}$$

$$\frac{\dot{\tau}\eta_1}{\mu_2\mu_1} = \frac{\eta_1}{\mu_1}\frac{\eta_2}{\mu_2}\ddot{\gamma}_2 + \frac{\eta_1}{\mu_1}\dot{\gamma}_2 \tag{14}$$

$$\frac{\dot{\tau}}{\mu_e}\left(\frac{\eta_1}{\mu_1} + \frac{\eta_2}{\mu_2}\right) = \left(\frac{\eta_1}{\mu_1} + \frac{\eta_2}{\mu_2}\right)\dot{\gamma}_e \tag{15}$$

Subsequent summation of Eqs. (12)–(15), together with consideration of Eq. (3) in form of $\dot{\gamma} = \dot{\gamma}_e + \dot{\gamma}_1 + \dot{\gamma}_2$, yields an expression free from $\dot{\gamma}_1$ and $\dot{\gamma}_2$, namely

$$\tau\left(\frac{1}{\mu_e} + \frac{1}{\mu_1} + \frac{1}{\mu_2}\right) + \dot{\tau}\left[\frac{\eta_1}{\mu_1}\left(\frac{1}{\mu_2} + \frac{1}{\mu_e}\right) + \frac{\eta_2}{\mu_2}\left(\frac{1}{\mu_1} + \frac{1}{\mu_e}\right)\right] = \gamma + \left(\frac{\eta_1}{\mu_1} + \frac{\eta_2}{\mu_2}\right)\dot{\gamma} + \frac{\eta_1\eta_2}{\mu_1\mu_2}(\ddot{\gamma}_1 + \ddot{\gamma}_2) \tag{16}$$

Finally, second-order derivatives $\ddot{\gamma}_1$ and $\ddot{\gamma}_2$ are eliminated from Eq. (16). Therefore, the second-order time derivative of Eq. (11) is multiplied with $(\frac{\eta_1\eta_2}{\mu_1\mu_2})$, yielding

$$\frac{\ddot{\tau}\eta_1\eta_2}{\mu_e\mu_1\mu_2} = \frac{\eta_1\eta_2}{\mu_1\mu_2}\ddot{\gamma}_e \tag{17}$$

Summing up Eqs. (16) and (17) while considering Eq. (3) in form of $\ddot{\gamma} = \ddot{\gamma}_e + \ddot{\gamma}_1 + \ddot{\gamma}_2$, then yields the sought constitutive relation between τ and γ

$$\tau\left(\frac{1}{\mu_e} + \frac{1}{\mu_1} + \frac{1}{\mu_2}\right) + \dot{\tau}\left[\frac{\eta_1}{\mu_1}\left(\frac{1}{\mu_2} + \frac{1}{\mu_e}\right) + \frac{\eta_2}{\mu_2}\left(\frac{1}{\mu_1} + \frac{1}{\mu_e}\right)\right] + \ddot{\tau}\frac{\eta_1\eta_2}{\mu_1\mu_2}\left(\frac{1}{\mu_e}\right) = \gamma + \left(\frac{\eta_1}{\mu_1} + \frac{\eta_2}{\mu_2}\right)\dot{\gamma} + \frac{\eta_1\eta_2}{\mu_1\mu_2}\ddot{\gamma} \tag{18}$$

The same strategy can be applied in order to derive a constitutive relation between τ and γ for a chain model containing three Kelvin-Voigt units ($N = 3$), (Fig. 3). The elementary stress-strain relations of the Kelvin-Voigt units and the one of the additional spring are combined, such that γ_1, γ_2, γ_3, and γ_e are eliminated. The resulting expression involves terms containing $\dot{\gamma}_1, \dot{\gamma}_2$, and $\dot{\gamma}_3$. They are eliminated by constructing a suitable linear combination of the aforementioned expression and the first-order time derivatives of the elementary stress-strain relations. This will introduce terms containing $\ddot{\gamma}_1$, $\ddot{\gamma}_2$, and $\ddot{\gamma}_3$, into the new expression arising from the aforementioned linear combination. By constructing a suitable linear combination of this new expression and the second-order time derivatives of the aforementioned stress-strain relations, $\ddot{\gamma}_1, \ddot{\gamma}_2$, and $\ddot{\gamma}_3$ can be eliminated as well, but third-order terms appear, $\dddot{\gamma}_1$, $\dddot{\gamma}_2$, and $\dddot{\gamma}_3$. They can be eliminated by constructing a suitable linear combination with the third-order time derivative of the elementary stress-strain relation of the additional spring. In the end, the following third-order differential equation in τ and γ is obtained:

$$\tau\left(\frac{1}{\mu_e} + \frac{1}{\mu_1} + \frac{1}{\mu_2} + \frac{1}{\mu_3}\right) + \dot{\tau}\left[\frac{\eta_1}{\mu_1}\left(\frac{1}{\mu_2} + \frac{1}{\mu_3} + \frac{1}{\mu_e}\right) + \frac{\eta_2}{\mu_2}\left(\frac{1}{\mu_1} + \frac{1}{\mu_3} + \frac{1}{\mu_e}\right) + \frac{\eta_3}{\mu_3}\left(\frac{1}{\mu_1} + \frac{1}{\mu_2} + \frac{1}{\mu_e}\right)\right] + \ddot{\tau}\left[\frac{\eta_1\eta_2}{\mu_1\mu_2}\left(\frac{1}{\mu_e} + \frac{1}{\mu_3}\right) + \frac{\eta_1\eta_3}{\mu_1\mu_3}\left(\frac{1}{\mu_e} + \frac{1}{\mu_2}\right) + \frac{\eta_2\eta_3}{\mu_2\mu_3}\left(\frac{1}{\mu_e} + \frac{1}{\mu_1}\right)\right] + \dddot{\tau}\frac{\eta_1\eta_2\eta_3}{\mu_1\mu_2\mu_3}\left(\frac{1}{\mu_e}\right) = \gamma + \left(\frac{\eta_1}{\mu_1} + \frac{\eta_2}{\mu_2} + \frac{\eta_3}{\mu_3}\right)\dot{\gamma} + \left(\frac{\eta_1\eta_2}{\mu_1\mu_2} + \frac{\eta_2\eta_3}{\mu_2\mu_3} + \frac{\eta_1\eta_3}{\mu_1\mu_3}\right)\ddot{\gamma} + \frac{\eta_1\eta_2\eta_3}{\mu_1\mu_2\mu_3}\dddot{\gamma} \tag{19}$$

The general structure of constitutive τ-γ relations for chain models containing N Kelvin Voigt units can be identified by comparing the τ-γ relations for one, two, and three Kelvin Voigt units, respectively, see Eqs. (8), (18), and (19). Accordingly, it appears that the first-order derivative of the strain, $\dot{\gamma}$, is always multiplied with the sum over all characteristic times η_i/μ_i, with $i = 1, 2, \ldots, N$. The second-order derivative of the strain, $\ddot{\gamma}$, is always multiplied with the sum over all possible products of two different characteristic times. The third-order derivative of the strain, $\dddot{\gamma}$, is always multiplied with the sum over all possible products of three different characteristic times. This clarifies the general structure: the nth-order derivative of the strain is multiplied with the sum over all possible products of n different characteristic times. The coefficients multiplied with the stress and

stress derivatives are just slightly more complex: The stress, τ, is always multiplied with the sum over all reciprocal shear stiffness values. The first-order derivative of the stress, $\dot{\tau}$, is always multiplied with the sum over all products of each characteristic time η_i/μ_i and a corresponding constant being equal to the sum over all reciprocal shear stiffness values minus $1/\mu_i$. The second-order derivative of the stress, $\ddot{\tau}$, is always multiplied with the sum over all possible products of two different characteristic times, $\eta_i\eta_j/(\mu_i\mu_j)$, whereby $i \neq j$, and corresponding constants which are equal to the sum over all reciprocal shear stiffness values minus $(1/\mu_i + 1/\mu_j)$. The third-order derivative of the stress, $\dddot{\tau}$, is always multiplied with the sum over all possible products of three different characteristic times, $\eta_i\eta_j\eta_k/(\mu_i\mu_j\mu_k)$, whereby $i \neq j$, $i \neq k$, $j \neq k$, and corresponding constants which are equal to the sum over all reciprocal shear stiffness values minus $(1/\mu_i + 1/\mu_j + 1/\mu_k)$. This clarifies the general structure: the nth-order derivative of the stress is multiplied with the sum over all possible products of n different characteristic times, and corresponding constants being equal to the sum over all reciprocal shear stiffness values minus the sum over all those reciprocal shear stiffness values which also show up in the products of the characteristic times. In conclusion, the mathematical format of the general τ-γ relation for a chain model with N Kelvin-Voigt units reads as

$$\left(\frac{1}{\mu_e}+\sum_{l=1}^{N}\frac{1}{\mu_l}\right)\tau+\sum_{n=1}^{N}\left(\sum_{i_1=1}^{N-n+1}\cdots\left(\sum_{i_a=i_{a-1}+1}^{N-(n-a)+1}\cdots\left(\sum_{i_n=i_{n-1}+1}^{N}\left(\left(\left(\frac{1}{\mu_e}+\sum_{l=1}^{N}\frac{1}{\mu_l}\right)-\sum_{j\in\{i_1,\ldots,i_n\}}\frac{1}{\mu_j}\right)\left(\prod_{k\in\{i_1,\ldots,i_n\}}\frac{\eta_k}{\mu_k}\right)\right)\right)\cdots\right)\cdots\right)\frac{\partial^n\tau}{\partial t^n}$$
$$=$$
$$\gamma+\sum_{n=1}^{N}\left(\sum_{i_1=1}^{N-n+1}\cdots\left(\sum_{i_a=i_{a-1}+1}^{N-(n-a)+1}\cdots\left(\sum_{i_n=i_{n-1}+1}^{N}\left(\prod_{j\in\{i_1,\ldots,i_n\}}\frac{\eta_j}{\mu_j}\right)\right)\cdots\right)\cdots\right)\frac{\partial^n\gamma}{\partial t^n} \tag{20}$$

see also Eq. (68) in the Appendix for a more expanded form of Eq. (20).

Maxwell Chain Models

Here, we consider Maxwell chain models consisting of N Maxwell units in parallel with an additional elastic spring (Fig. 4). Again, such chain models are considered to represent a piece of material subjected to pure shear, see Eqs. (1) and (2); or more generally speaking, they represent a material creeping only in shear mode, under any general loading condition.

The overall shear stress of the rheological model, $\tau = \Sigma_{xz}$ according to Eq. (1), can be decomposed additively into the stresses transferred through the individual Maxwell units $(\tau_I, \tau_{II}, \ldots, \tau_N)$ and into the one transferred through the elastic spring (τ_E)

$$\tau = \tau_E + \sum_{i=I}^{N}\tau_i \tag{21}$$

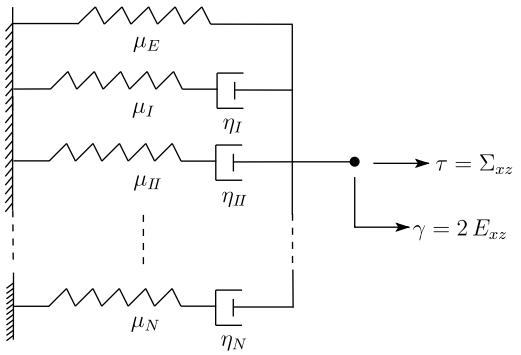

Fig. 4. Maxwell chain, used to model time-dependent behavior under pure shear; see Eqs. (1) and (2), with $\Sigma_{xz} = \tau$ and $2E_{xz} = \gamma$

In turn, the overall shear deformation $\gamma = 2E_{xz}$ according to Eq. (2), is the same for all N Maxwell units ($\gamma_I = \gamma_{II} = \cdots = \gamma_N = \gamma$) and for the elastic spring ($\gamma_E = \gamma$), such that

$$\gamma = \gamma_I = \gamma_{II} = \cdots = \gamma_N = \gamma_E \tag{22}$$

The shear deformation of the ith Maxwell unit can be decomposed into the shear deformation of the spring, γ_I^{μ}, and into the shear deformation of the dashpot, γ_I^{η}

$$\gamma = \gamma_i^{\mu} + \gamma_i^{\eta} \qquad i = I, II, \ldots, N \tag{23}$$

The derivation of a constitutive relation between shear stress $\tau = \Sigma_{xz}$ and shear strain $\gamma = 2E_{xz}$, see Eqs. (1) and (2) and Fig. 4, requires individual constitutive laws for all involved rheological devices. Denoting the stiffness of the additional elastic spring as μ_E, the stiffnesses of the Maxwell springs as $\mu_I, \mu_{II}, \ldots, \mu_N$, and the dashpot viscosities as $\eta_I, \eta_{II}, \ldots, \eta_N$, see Fig. 4, the individual constitutive laws read, in analogy to Eq. (6), as

$$\left.\begin{aligned}\tau_i &= \mu_i\gamma_i^{\mu}\\ \tau_i &= \eta_i\dot{\gamma}_i^{\eta}\end{aligned}\right\} \qquad i = I, II, \ldots, N \quad \tau_E = \mu_E\gamma_E \tag{24}$$

The sought constitutive relation between τ and γ is obtained by constructing linear combinations of Eqs. (21)–(24) and their time derivatives, yielding, for a chain model with one Maxwell unit ($N = I$), see (Shahidi et al. 2015b)

$$\tau + \dot{\tau}\frac{\eta_I}{\mu_I} = \gamma\mu_E + \dot{\gamma}\frac{\eta_I}{\mu_I}(\mu_E + \mu_I) \tag{25}$$

In agreement with our current focus on more than one interface size and/or viscosity, we continue with the derivation of the constitutive τ-γ relation for a chain model with two Maxwell units ($N = II$), (Fig. 5). In this context, it is beneficial to derive elementary stress-strain relations for the individual Maxwell units by specifying the time derivative of Eqs. (23) and (24) for the spring and dashpot

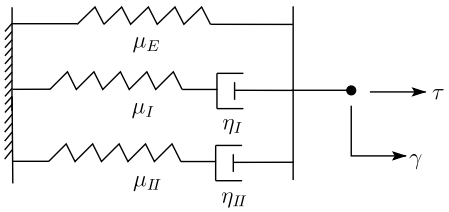

Fig. 5. Maxwell chain with two units ($N = 2$); see Eq. (35) for the governing differential equation

laws, and by multiplying the resulting expressions with the viscosity of the involved dashpot, yielding

$$\tau_I + \dot{\tau}_I \frac{\eta_I}{\mu_I} = \dot{\gamma}\eta_I \tag{26}$$

$$\tau_{II} + \dot{\tau}_{II} \frac{\eta_{II}}{\mu_{II}} = \dot{\gamma}\eta_{II} \tag{27}$$

By analogy, the shear deformation γ_E appearing in the spring law of the additional spring, see Eq. (24), can be set equal to γ, according to Eq. (22), so that we obtain

$$\tau_E = \mu_E \gamma \tag{28}$$

Summing up Eqs. (26)–(28) and consideration of Eq. (21) allows for elimination of τ_I, τ_{II}, and τ_E, yielding

$$\tau + \dot{\tau}_I \frac{\eta_I}{\mu_I} + \dot{\tau}_{II} \frac{\eta_{II}}{\mu_{II}} = \gamma\mu_E + \dot{\gamma}(\eta_I + \eta_{II}) \tag{29}$$

Next, first-order time derivatives $\dot{\tau}_I$ and $\dot{\tau}_{II}$ are eliminated by constructing linear combinations of Eq. (29) with the first-order time derivatives of Eqs. (26), (27), and (28), whereby the latter derivatives are multiplied with η_{II}/μ_{II}, with η_I/μ_I, and with $\eta_I/\mu_I + \eta_{II}/\mu_{II}$, respectively

$$\dot{\tau}_I \frac{\eta_{II}}{\mu_{II}} + \ddot{\tau}_I \frac{\eta_I \eta_{II}}{\mu_I \mu_{II}} = \ddot{\gamma} \frac{\eta_I \eta_{II}}{\mu_{II}} \tag{30}$$

$$\dot{\tau}_{II} \frac{\eta_I}{\mu_I} + \ddot{\tau}_{II} \frac{\eta_I \eta_{II}}{\mu_I \mu_{II}} = \ddot{\gamma} \frac{\eta_I \eta_{II}}{\mu_I} \tag{31}$$

$$\dot{\tau}_E \left(\frac{\eta_I}{\mu_I} + \frac{\eta_{II}}{\mu_{II}} \right) = \dot{\gamma}\mu_E \left(\frac{\eta_I}{\mu_I} + \frac{\eta_{II}}{\mu_{II}} \right) \tag{32}$$

Summing up Eqs. (29)–(32) and consideration of Eq. (21) in the form of $\dot{\tau} = \dot{\tau}_E + \dot{\tau}_I + \dot{\tau}_{II}$, yields

$$\tau + \dot{\tau}\left(\frac{\eta_I}{\mu_I} + \frac{\eta_{II}}{\mu_{II}} \right) + (\ddot{\tau}_I + \ddot{\tau}_{II}) \frac{\eta_I \eta_{II}}{\mu_I \mu_{II}}$$
$$=$$
$$\gamma\mu_E + \dot{\gamma}\left[\frac{\eta_I}{\mu_I}(\mu_E + \mu_I) + \frac{\eta_{II}}{\mu_{II}}(\mu_E + \mu_{II}) \right] + \ddot{\gamma} \frac{\eta_I \eta_{II}}{\mu_I \mu_{II}} (\mu_I + \mu_{II}) \tag{33}$$

Finally, the second-order time derivatives $\ddot{\tau}_I$ and $\ddot{\tau}_{II}$ are eliminated by constructing a linear combination of Eq. (33) with the second-order time derivative of Eq. (28), whereby the latter is multiplied with $(\frac{\eta_I \eta_{II}}{\mu_I \mu_{II}})$, i.e.

$$\ddot{\tau}_E \frac{\eta_I \eta_{II}}{\mu_I \mu_{II}} = \ddot{\gamma}\mu_E \frac{\eta_I \eta_{II}}{\mu_I \mu_{II}} \tag{34}$$

Summing up Eqs. (33) and (34) and consideration of Eq. (23) in the form of $\ddot{\tau} = \ddot{\tau}_E + \ddot{\tau}_I + \ddot{\tau}_{II}$ yields the sought constitutive relation between τ and γ

$$\tau + \dot{\tau}\left(\frac{\eta_I}{\mu_I} + \frac{\eta_{II}}{\mu_{II}} \right) + \ddot{\tau} \frac{\eta_I \eta_{II}}{\mu_I \mu_{II}}$$
$$=$$
$$\gamma\mu_E + \dot{\gamma}\left[\frac{\eta_I}{\mu_I}(\mu_E + \mu_I) + \frac{\eta_{II}}{\mu_{II}}(\mu_E + \mu_{II}) \right] + \ddot{\gamma} \frac{\eta_I}{\mu_I} \frac{\eta_{II}}{\mu_{II}} (\mu_E + \mu_I + \mu_{II}) \tag{35}$$

The same strategy can be applied to derive a constitutive relation between τ and γ for a chain model containing three Maxwell units ($N = III$), (Fig. 6). The elementary stress-strain relations of the Maxwell units and the one of the additional spring are combined, such that τ_I, τ_{II}, τ_{III}, and τ_E are eliminated. The resulting expression contains terms in $\dot{\tau}_I, \dot{\tau}_{II}$, and $\dot{\tau}_{III}$. They are eliminated by constructing a suitable linear combination with the first-order time derivatives of the elementary stress-strain relations. This will introduce terms containing $\ddot{\tau}_I$, $\ddot{\tau}_{II}$, and $\ddot{\tau}_{III}$. They are eliminated by constructing a suitable linear combination with the second-order time derivatives of the aforementioned stress-strain relations. This will introduce terms containing $\dddot{\tau}_I$, $\dddot{\tau}_{II}$, and $\dddot{\tau}_{III}$, and they can be eliminated by constructing a suitable linear combination with the third-order time derivative of the elementary stress-strain relation of the additional spring. In the end, the following third-order differential equation in τ and γ is obtained:

$$\tau + \dot{\tau}\left(\frac{\eta_I}{\mu_I} + \frac{\eta_{II}}{\mu_{II}} + \frac{\eta_{III}}{\mu_{III}} \right) + \ddot{\tau}\left(\frac{\eta_I \eta_{II}}{\mu_I \mu_{II}} + \frac{\eta_I \eta_{III}}{\mu_I \mu_{III}} + \frac{\eta_{II} \eta_{III}}{\mu_{II} \mu_{III}} \right) + \dddot{\tau}\left(\frac{\eta_I \eta_{II} \eta_{III}}{\mu_I \mu_{II} \mu_{III}} \right)$$
$$=$$
$$\gamma\mu_E + \dot{\gamma}\left[\frac{\eta_I}{\mu_I}(\mu_E + \mu_I) + \frac{\eta_{II}}{\mu_{II}}(\mu_E + \mu_{II}) + \frac{\eta_{III}}{\mu_{III}}(\mu_E + \mu_{III}) \right]$$
$$+$$
$$\ddot{\gamma}\left[\frac{\eta_I}{\mu_I} \frac{\eta_{II}}{\mu_{II}}(\mu_E + \mu_I + \mu_{II}) + \frac{\eta_I}{\mu_I} \frac{\eta_{III}}{\mu_{III}}(\mu_E + \mu_I + \mu_{III}) + \frac{\eta_{II}}{\mu_{II}} \frac{\eta_{III}}{\mu_{III}}(\mu_E + \mu_{II} + \mu_{III}) \right]$$
$$+$$
$$\dddot{\gamma} \frac{\eta_I}{\mu_I} \frac{\eta_{II}}{\mu_{II}} \frac{\eta_{III}}{\mu_{III}} (\mu_E + \mu_I + \mu_{II} + \mu_{III}) \tag{36}$$

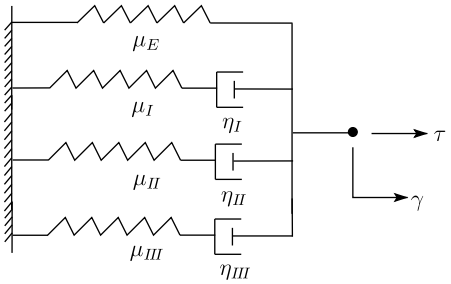

Fig. 6. Maxwell chain with three units ($N = 3$); see Eq. (36) for the governing differential equation

The general structure of constitutive τ-γ relations for chain models containing N Maxwell units can be identified from comparing the τ-γ relations of one, two, and three Maxwell units, respectively, see Eqs. (25), (35), and (36). Accordingly, it appears that the first-order derivative of the stress, $\dot{\tau}$, is always multiplied with the sum over all characteristic times η_i/μ_i, $i = I, II, \ldots, N$. The second-order derivative of the stress, $\ddot{\tau}$, is always multiplied with the sum over all possible products of two different characteristic times. The third-order derivative of the stress, $\dddot{\tau}$, is always multiplied with the sum over all possible products of three different characteristic times. This clarifies the general structure: the nth-order derivative of the stress is multiplied with the sum over all possible products of n different characteristic times. The strain, γ, is always multiplied with the shear stiffness of the additional spring. The first-order derivative of the strain, $\dot{\gamma}$, is always multiplied with the sum over all products of each characteristic time, η_i/μ_i, and a corresponding sum of stiffnesses $(\mu_E + \mu_i)$. The second-order derivative of the strain, $\ddot{\gamma}$, is always multiplied with the sum over all possible products of two different characteristic times, $\eta_i\eta_j/(\mu_i\mu_j)$, whereby $i \neq j$, and corresponding sums of stiffnesses read as $(\mu_E + \mu_i + \mu_j)$. The third-order derivative of the stress, $\dddot{\gamma}$, is always multiplied with the sum over all possible products of three different characteristic times, $\eta_i\eta_j\eta_k/(\mu_i\mu_j\mu_k)$, whereby $i \neq j$, $i \neq k$, and $j \neq k$, and factors in the form of stiffness sums $(\mu_E + \mu_i + \mu_j + \mu_k)$. This clarifies the general structure: the nth-order derivative of the strain is multiplied with the sum over all possible products of n different characteristic times and corresponding constants being equal to the sum of the shear stiffness of the additional spring plus all shear stiffnesses, which also show up in the products of the characteristic times. Accordingly, the mathematical format of the general τ-γ relation for a chain model with N Maxwell units reads as

$$\tau + \sum_{n=I}^{N}\left(\sum_{i_I=I}^{N-n+I}\cdots\left(\sum_{i_a=i_{a-I}+I}^{N-(n-a)+I}\cdots\left(\sum_{i_n=i_{n-I}+I}^{N}\left(\prod_{j\in\{i_I,\ldots,i_n\}}\frac{\eta_j}{\mu_j}\right)\right)\cdots\right)\cdots\right)\frac{\partial^n\tau}{\partial t^n} = \mu_E\gamma$$
$$+\sum_{n=I}^{N}\left(\sum_{i_I=I}^{N-n+I}\cdots\left(\sum_{i_a=i_{a-I}+I}^{N-(n-a)+I}\cdots\left(\sum_{i_n=i_{n-I}+I}^{N}\left(\left(\mu_E+\sum_{j\in\{i_I,\ldots,i_n\}}\mu_j\right)\left(\prod_{k\in\{i_I,\ldots,i_n\}}\frac{\eta_k}{\mu_k}\right)\right)\right)\cdots\right)\cdots\right)\frac{\partial^n\gamma}{\partial t^n} \tag{37}$$

see also Eq. (69) in the Appendix for a more expanded form of Eq. (37).

Matrix-Interface Representation and Constitutive Relations

Here, we consider matrix-inclusion composites consisting of one solid phase and of N parallel interface phases, differing by viscosity and size, representing together the entity of all viscous fluid layers within the investigated material volume (Fig. 7). These composite materials are subjected to pure shear, which is aligned with the interface orientation, see Eqs. (1) and (2), and the solid phase exhibits linear elastic behavior characterized by an isotropic stiffness tensor $\underline{\underline{\underline{\underline{C}}}}_s$.

In more symbolic detail, each interface phase is characterized by a specific interface radius a_i and a specific interface viscosity η_i^{int}, with $i = 1,2,\ldots,N$. In addition, we consider that molecular ordering-related joining forces prevent the interfaces from opening, so that displacement jumps in interface normal direction $\underline{e}_z$ vanish. The component of the traction vector acting in the interface plane, $T_{i,x}$, is related, by a linear viscous law, to the rate of the average in-plane displacement jump, $[\![\dot{\xi}]\!]_{i,x}$

$$T_{i,x} = \eta_i^{\text{int}}[\![\dot{\xi}]\!]_{i,x} \quad i = 1,2,\ldots,N \tag{38}$$

The derivation of a differential equation describing the constitutive behavior of the studied composite in terms of macroscopic stress Σ_{xz} and strain E_{xz} is based on the macroscopic poromechanical state equation and on concentration-influence relations, as described next.

The macroscopic state equation, expressing the macrostress $\underline{\underline{\Sigma}}$ as a function of the macrostrain $\underline{\underline{E}}$ and of all interface traction vectors $\underline{T}_i$ reads as (Shahidi et al. 2014)

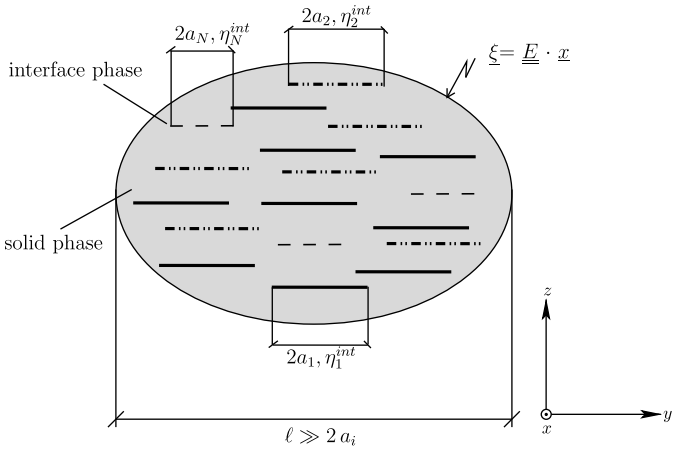

Fig. 7. Matrix-interface composite including N families of 2D flat, parallel, spherical interfaces; 2D sketch of 3D representative volume elements

$$\underline{\underline{\Sigma}} = \underline{\underline{\underline{\underline{C}}}}_{\text{hom}} : \underline{\underline{E}} + \sum_{i=1}^{N} \underline{\underline{\underline{B}}}_i \cdot \underline{T}_i \tag{39}$$

where $\underline{\underline{\underline{\underline{C}}}}_{\text{hom}}$ denotes the homogenized stiffness tensor of the studied composite, and $\underline{\underline{\underline{B}}}_i$ denotes a Biot-type tensor quantifying the influence of interface traction vector $\underline{T}_i$ on the macrostress $\underline{\underline{\Sigma}}$ provided that the macrostrain $\underline{\underline{E}}$ and all the other interface traction vectors are equal to zero. Specifying Eq. (39) for the matrix-interface composite shown in Fig. 7, and for loading in terms of pure macroscopic shear according to Eqs. (1) and (2), allows for extracting the following scalar equation linking shear stress Σ_{xz}, shear strain E_{xz}, and the in-plane interface traction vector components $T_{i,x}$, $i = 1,2,\ldots,N$ (Shahidi et al. 2014)

$$\Sigma_{xz} = \frac{3\mu_s(2-\nu_s)}{3(2-\nu_s)+16(1-\nu_s)\sum_{i=1}^{N} d_i} 2E_{xz} + \frac{16(1-\nu_s)\sum_{i=1}^{N} T_{i,x} d_i}{3(2-\nu_s)+16(1-\nu_s)\sum_{i=1}^{N} d_i} \tag{40}$$

In Eq. (40), μ_s and ν_s stand for the shear modulus and for Poisson's ratio of the isotropic elastic solid matrix.

The concentration-influence relation expressing the dislocation vector $[\![\underline{\xi}]\!]_i$ as a function of the macrostrain $\underline{\underline{E}}$ and of all interface traction vectors $\underline{T}_j$ reads as (Shahidi et al. 2014)

$$[\![\underline{\xi}]\!]_i = \underline{\underline{\underline{A}}}_i : \underline{\underline{E}} + \sum_{j=1}^{N} \underline{\underline{\underline{D}}}_{ij} \cdot \underline{T}_j \tag{41}$$

where $\underline{\underline{\underline{A}}}_i$ denotes a concentration tensor quantifying the influence of macrostrain $\underline{\underline{E}}$ on the dislocation vector $[\![\underline{\xi}]\!]_i$ provided that all interface traction vectors $\underline{T}_j$ vanish; and $\underline{\underline{\underline{D}}}_{ij}$ stands for an influence tensor quantifying the influence of the interface traction vector $\underline{T}_j$ on the dislocation vector $[\![\underline{\xi}]\!]_i$ provided that macrostrain $\underline{\underline{E}}$ and all the other interface traction vectors vanish. Specifying Eq. (41) for the matrix-interface composite shown in Fig. 7, and for loading in terms of pure macroscopic shear according to Eqs. (1) and (2), allows for extracting a scalar equation linking in-plane dislocation $[\![\xi]\!]_{i,x}$, the shear strain E_{xz}, and the in-plane interface traction vector components $T_{j,x}$ (Shahidi et al. 2014). It reads as

$$[\![\xi]\!]_{i,x} = \frac{8(1-\nu_s)a_i}{\pi[3(2-\nu_s)+16(1-\nu_s)\sum_{j=1}^{N} d_j]} \times \left[2E_{xz} - \frac{T_{i,x}}{\mu_s} + \frac{16(1-\nu_s)}{3\mu_s(2-\nu_s)} \sum_{j=1}^{N} d_j (T_{j,x} - T_{i,x})\right] \tag{42}$$

The sought differential equation in Σ_{xz} and E_{xz} is derived by means of linearly combining Eqs. (38), (40), and (42), as well as their time derivatives. For the special case of one interface phase, $N = 1$, macroscopic state equation Eq. (40) and concentration-influence relation Eq. (42) are given in Eqs. (31) and (34) of the companion paper (Shahidi et al. 2015b), and the sought differential equation is obtained as

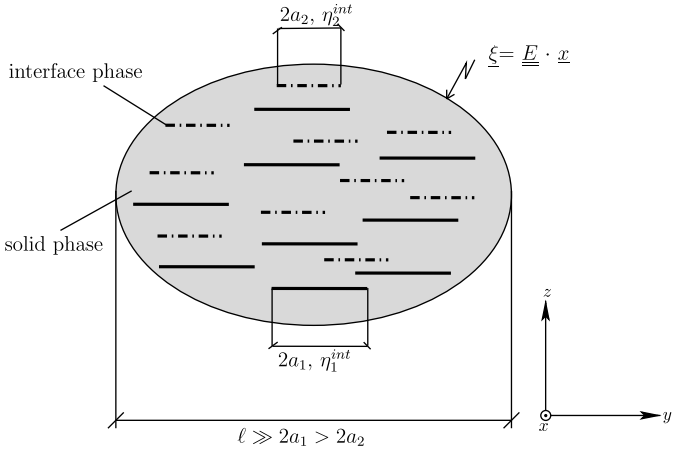

Fig. 8. Matrix-interface composite with two families of 2D flat, parallel, spherical interfaces; 2D sketch of 3D representative volume elements

$$\dot{\Sigma}_{xz} \frac{8a_1\eta_1^{\text{int}}(1-\nu_s)}{3\pi(2-\nu_s)\mu_s}\left(\frac{1}{\mu_s}\right) + \Sigma_{xz}\left(\frac{1}{\mu_s} + \frac{1}{\mu_s}\frac{16d_1(1-\nu_s)}{3(2-\nu_s)}\right) = 2\dot{E}_{xz}\frac{8a_1\eta_1^{\text{int}}(1-\nu_s)}{3\pi(2-\nu_s)\mu_s}\left(\frac{1}{\mu_s}\right) + 2E_{xz} \tag{43}$$

Next, we analyze the more general case of two interface phases ($N = 2$), (Fig. 8). Specifying the macroscopic state equation, Eq. (40), for $N = 2$ yields

$$\Sigma_{xz} = \frac{3\mu_s(2-\nu_s)}{3(2-\nu_s)+16(d_1+d_2)(1-\nu_s)} 2E_{xz} + \frac{16(1-\nu_s)(T_{1,x}d_1 + T_{2,x}d_2)}{3(2-\nu_s)+16(d_1+d_2)(1-\nu_s)} \tag{44}$$

and specifying the concentration-influence relation Eq. (42) for $N = 2$ delivers

$$[\![\xi]\!]_{1,x} = \frac{8(1-\nu_s)a_1}{\pi[3(2-\nu_s)+16(1-\nu_s)(d_1+d_2)]} \times \left[2E_{xz} - \frac{T_{1,x}}{\mu_s} + \frac{16(1-\nu_s)}{3\mu_s(2-\nu_s)} d_2 (T_{2,x} - T_{1,x})\right] \tag{45}$$

$$[\![\xi]\!]_{2,x} = \frac{8(1-\nu_s)a_2}{\pi[3(2-\nu_s)+16(1-\nu_s)(d_1+d_2)]} \times \left[2E_{xz} - \frac{T_{2,x}}{\mu_s} + \frac{16(1-\nu_s)}{3\mu_s(2-\nu_s)} d_1 (T_{1,x} - T_{2,x})\right] \tag{46}$$

In order to derive the sought relation between Σ_{xz} and E_{xz}, we construct a linear combination of Eqs. (44), (45), and (46), whereby Eqs. (45) and (46) are multiplied with $2\mu_s\pi d_1/a_1$ and with $2\mu_s\pi d_2/a_2$, respectively, such that the interface tractions $T_{1,x}$ and $T_{2,x}$ are eliminated

$$\frac{2\mu_s\pi d_1}{a_1}[\![\xi]\!]_{1,x} + \frac{2\mu_s\pi d_2}{a_2}[\![\xi]\!]_{2,x} + \Sigma_{xz} = 2\mu_s E_{xz} \tag{47}$$

Interface tractions are re-introduced by taking the time derivative of Eq. (47) and considering Eq. (38), i.e., $[\![\dot{\xi}]\!]_{1,x} = T_{1,x}/\eta_1^{\text{int}}$ as well as $[\![\dot{\xi}]\!]_{2,x} = T_{2,x}/\eta_2^{\text{int}}$

$$\frac{2\mu_s\pi d_1}{a_1\eta_1^{\text{int}}}T_{1,x} + \frac{2\mu_s\pi d_2}{a_2\eta_2^{\text{int}}}T_{2,x} + \dot{\Sigma}_{xz} = 2\mu_s\dot{E}_{xz} \tag{48}$$

Next, we construct a linear combination of Eqs. (48), (45), and (46), whereby Eqs. (45) and (46), respectively, are multiplied with

$$-\frac{d_1[16(1-\nu_s)(a_1\eta_1^{\text{int}}d_2 + a_2\eta_2^{\text{int}}d_1) + 3a_2\eta_2^{\text{int}}(2-\nu_s)]\mu_s^2\pi^2}{4a_1^2\eta_1^{\text{int}}a_2\eta_2^{\text{int}}(1-\nu_s)} \tag{49}$$

and

$$-\frac{d_2[16(1-\nu_s)(a_1\eta_1^{\text{int}}d_2 + a_2\eta_2^{\text{int}}d_1) + 3a_1\eta_1^{\text{int}}(2-\nu_s)]\mu_s^2\pi^2}{4a_1\eta_1^{\text{int}}a_2^2\eta_2^{\text{int}}(1-\nu_s)} \tag{50}$$

respectively, such that again, interface tractions $T_{1,x}$ and $T_{2,x}$ are eliminated, yielding

$$\dot{\Sigma}_{xz} - \frac{d_1[16(1-\nu_s)(a_1\eta_1^{\text{int}}d_2+a_2\eta_2^{\text{int}}d_1)+3a_2\eta_2^{\text{int}}(2-\nu_s)]\mu_s^2\pi^2}{4a_1^2\eta_1^{\text{int}}a_2\eta_2^{\text{int}}(1-\nu_s)}[\![\xi]\!]_{1,x} - \frac{d_2[16(1-\nu_s)(a_1\eta_1^{\text{int}}d_2+a_2\eta_2^{\text{int}}d_1)+3a_1\eta_1^{\text{int}}(2-\nu_s)]\mu_s^2\pi^2}{4a_1\eta_1^{\text{int}}a_2^2\eta_2^{\text{int}}(1-\nu_s)}[\![\xi]\!]_{2,x} = 2\mu_s\dot{E}_{xz} - \frac{4(a_1\eta_1^{\text{int}}d_2+a_2\eta_2^{\text{int}}d_1)\pi\mu_s^2}{a_1\eta_1^{\text{int}}a_2\eta_2^{\text{int}}}E_{xz} \tag{51}$$

Interface tractions are re-introduced by taking the time derivative of Eq. (51) and considering Eq. (38), i.e., $[\![\dot{\xi}]\!]_{1,x} = T_{1,x}/\eta_1^{\text{int}}$ as well as $[\![\dot{\xi}]\!]_{2,x} = T_{2,x}/\eta_2^{\text{int}}$

$$\ddot{\Sigma}_{xz} - \frac{d_1[16(1-\nu_s)(a_1\eta_1^{\text{int}}d_2+a_2\eta_2^{\text{int}}d_1)+3a_2\eta_2^{\text{int}}(2-\nu_s)]\mu_s^2\pi^2}{4a_1^2(\eta_1^{\text{int}})^2a_2\eta_2^{\text{int}}(1-\nu_s)}T_{1,x} - \frac{d_2[16(1-\nu_s)(a_1\eta_1^{\text{int}}d_2+a_2\eta_2^{\text{int}}d_1)+3a_1\eta_1^{\text{int}}(2-\nu_s)]\mu_s^2\pi^2}{4a_1\eta_1^{\text{int}}a_2^2(\eta_2^{\text{int}})^2(1-\nu_s)}T_{2,x} = 2\mu_s\ddot{E}_{xz} - \frac{4(a_1\eta_1^{\text{int}}d_2+a_2\eta_2^{\text{int}}d_1)\pi\mu_s^2}{a_1\eta_1^{\text{int}}a_2\eta_2^{\text{int}}}\dot{E}_{xz} \tag{52}$$

The sought differential equation is finally obtained by constructing a linear combination of Eqs. (44), (48), and (52), whereby Eqs. (44) and (48), respectively, are multiplied with

$$\frac{[16(1-\nu_s)(a_1\eta_1^{\text{int}}d_2 + a_2\eta_2^{\text{int}}d_1) + 3a_1\eta_1^{\text{int}}(2-\nu_s) + 3a_2\eta_2^{\text{int}}(2-\nu_s)]\mu_s\pi}{8a_1\eta_1^{\text{int}}a_2\eta_2^{\text{int}}(1-\nu_s)} \tag{53}$$

and

$$\frac{3[16(1-\nu_s)(d_1+d_2) + 3(2-\nu_s)]\pi^2\mu_s^2(2-\nu_s)}{64a_1\eta_1^{\text{int}}a_2\eta_2^{\text{int}}(1-\nu_s)^2} \tag{54}$$

respectively. Re-arranging terms in the resulting expression, such that $2E_{xz}$ is multiplied with a coefficient being equal to 1, delivers

$$\ddot{\Sigma}_{xz}\left[\frac{8a_1\eta_1^{\text{int}}(1-\nu_s)}{3\pi(2-\nu_s)\mu_s}\frac{8a_2\eta_2^{\text{int}}(1-\nu_s)}{3\pi(2-\nu_s)\mu_s}\left(\frac{1}{\mu_s}\right)\right] + \dot{\Sigma}_{xz}\left[\frac{8a_1\eta_1^{\text{int}}(1-\nu_s)}{3\pi(2-\nu_s)\mu_s}\left(\frac{1}{\mu_s}+\frac{1}{\mu_s}\frac{16d_2(1-\nu_s)}{3(2-\nu_s)}\right) + \frac{8a_2\eta_2^{\text{int}}(1-\nu_s)}{3\pi(2-\nu_s)\mu_s}\left(\frac{1}{\mu_s}+\frac{1}{\mu_s}\frac{16d_1(1-\nu_s)}{3(2-\nu_s)}\right)\right] + \Sigma_{xz}\left(\frac{1}{\mu_s}+\frac{1}{\mu_s}\frac{16d_1(1-\nu_s)}{3(2-\nu_s)}+\frac{1}{\mu_s}\frac{16d_2(1-\nu_s)}{3(2-\nu_s)}\right) = 2\ddot{E}_{xz}\left[\frac{8a_1\eta_1^{\text{int}}(1-\nu_s)}{3\pi(2-\nu_s)\mu_s}\frac{8a_2\eta_2^{\text{int}}(1-\nu_s)}{3\pi(2-\nu_s)\mu_s}\right] + 2\dot{E}_{xz}\left[\frac{8a_1\eta_1^{\text{int}}(1-\nu_s)}{3\pi(2-\nu_s)\mu_s}+\frac{8a_2\eta_2^{\text{int}}(1-\nu_s)}{3\pi(2-\nu_s)\mu_s}\right] + 2E_{xz} \tag{55}$$

The same strategy can be applied to derive a constitutive relation between Σ_{xz} and $2E_{xz}$ for a matrix-inclusion composite containing three interface phases ($N = 3$), (Fig. 9). The macroscopic poroelasticity-like state equation, Eq. (40), and the concentration-influence relations, Eq. (42), are combined, such that interface tractions $T_{1,x}$, $T_{2,x}$, and $T_{3,x}$ are eliminated. This results in an equation containing Σ_{xz}, $2E_{xz}$, $[\![\xi]\!]_{1,x}$, $[\![\xi]\!]_{2,x}$, and $[\![\xi]\!]_{3,x}$. Taking the time derivative of this equation and using the viscous law, Eq. (38), delivers an equation containing $\dot{\Sigma}_{xz}$, $2\dot{E}_{xz}$, $T_{1,x}$, $T_{2,x}$, and $T_{3,x}$. From this equation, the interface tractions are eliminated by constructing a suitable linear combination with the concentration-influence relations. The result is an expression containing $\dot{\Sigma}_{xz}$, $2\dot{E}_{xz}$, $2E_{xz}$, $[\![\xi]\!]_{1,x}$, $[\![\xi]\!]_{2,x}$, and $[\![\xi]\!]_{3,x}$. Taking the time derivative of this equation and using the viscous law Eq. (38) delivers an equation containing $\ddot{\Sigma}_{xz}$, $2\ddot{E}_{xz}$, $2\dot{E}_{xz}$, $T_{1,x}$, $T_{2,x}$, and $T_{3,x}$. From this equation, the interface tractions are eliminated by constructing a suitable linear combination with the concentration-influence relations. The result is an expression containing $\ddot{\Sigma}_{xz}$, $2\ddot{E}_{xz}$, $2\dot{E}_{xz}$, $2E_{xz}$, $[\![\xi]\!]_{1,x}$, $[\![\xi]\!]_{2,x}$, and $[\![\xi]\!]_{3,x}$. Taking the time derivative of this equation and using the viscous law Eq. (38) delivers an equation containing $\dddot{\Sigma}_{xz}$, $2\dddot{E}_{xz}$, $2\ddot{E}_{xz}$, $2\dot{E}_{xz}$, $T_{1,x}$, $T_{2,x}$, and $T_{3,x}$. The sought differential equation is obtained from constructing a linear combination of the derived equations containing (1) Σ_{xz}, $2E_{xz}$, $T_{1,x}$, $T_{2,x}$, and $T_{3,x}$; (2) $\dot{\Sigma}_{xz}$, $2\dot{E}_{xz}$, $2E_{xz}$, $T_{1,x}$, $T_{2,x}$, and $T_{3,x}$; (3) $\ddot{\Sigma}_{xz}$, $2\ddot{E}_{xz}$, $2\dot{E}_{xz}$, $2E_{xz}$, $T_{1,x}$, $T_{2,x}$, and $T_{3,x}$; and (4) $\dddot{\Sigma}_{xz}$, $2\dddot{E}_{xz}$, $2\ddot{E}_{xz}$, $2\dot{E}_{xz}$, $T_{1,x}$, $T_{2,x}$, and $T_{3,x}$, with the aim to eliminate the interface tractions. This delivers

$$\dddot{\Sigma}_{xz}\left[\frac{8a_1\eta_1^{\text{int}}(1-\nu_s)}{3\pi(2-\nu_s)\mu_s}\frac{8a_2\eta_2^{\text{int}}(1-\nu_s)}{3\pi(2-\nu_s)\mu_s}\frac{8a_3\eta_3^{\text{int}}(1-\nu_s)}{3\pi(2-\nu_s)\mu_s}\left(\frac{1}{\mu_s}\right)\right]+\ddot{\Sigma}_{xz}\left[\frac{8a_1\eta_1^{\text{int}}(1-\nu_s)}{3\pi(2-\nu_s)\mu_s}\frac{8a_2\eta_2^{\text{int}}(1-\nu_s)}{3\pi(2-\nu_s)\mu_s}\left(\frac{1}{\mu_s}+\frac{1}{\mu_s}\frac{16d_3(1-\nu_s)}{3(2-\nu_s)}\right)\right.$$
$$\left.+\frac{8a_1\eta_1^{\text{int}}(1-\nu_s)}{3\pi(2-\nu_s)\mu_s}\frac{8a_3\eta_3^{\text{int}}(1-\nu_s)}{3\pi(2-\nu_s)\mu_s}\left(\frac{1}{\mu_s}+\frac{1}{\mu_s}\frac{16d_2(1-\nu_s)}{3(2-\nu_s)}\right)+\frac{8a_2\eta_2^{\text{int}}(1-\nu_s)}{3\pi(2-\nu_s)\mu_s}\frac{8a_3\eta_3^{\text{int}}(1-\nu_s)}{3\pi(2-\nu_s)\mu_s}\left(\frac{1}{\mu_s}+\frac{1}{\mu_s}\frac{16d_1(1-\nu_s)}{3(2-\nu_s)}\right)\right]$$
$$+\dot{\Sigma}_{xz}\left[\frac{8a_1\eta_1^{\text{int}}(1-\nu_s)}{3\pi(2-\nu_s)\mu_s}\left(\frac{1}{\mu_s}+\frac{1}{\mu_s}\frac{16d_2(1-\nu_s)}{3(2-\nu_s)}+\frac{1}{\mu_s}\frac{16d_3(1-\nu_s)}{3(2-\nu_s)}\right)+\frac{8a_2\eta_2^{\text{int}}(1-\nu_s)}{3\pi(2-\nu_s)\mu_s}\left(\frac{1}{\mu_s}+\frac{1}{\mu_s}\frac{16d_1(1-\nu_s)}{3(2-\nu_s)}+\frac{1}{\mu_s}\frac{16d_3(1-\nu_s)}{3(2-\nu_s)}\right)\right.$$
$$\left.+\frac{8a_3\eta_3^{\text{int}}(1-\nu_s)}{3\pi(2-\nu_s)\mu_s}\left(\frac{1}{\mu_s}+\frac{1}{\mu_s}\frac{16d_1(1-\nu_s)}{3(2-\nu_s)}+\frac{1}{\mu_s}\frac{16d_2(1-\nu_s)}{3(2-\nu_s)}\right)\right]+\Sigma_{xz}\left(\frac{1}{\mu_s}+\frac{1}{\mu_s}\frac{16d_1(1-\nu_s)}{3(2-\nu_s)}+\frac{1}{\mu_s}\frac{16d_2(1-\nu_s)}{3(2-\nu_s)}+\frac{1}{\mu_s}\frac{16d_3(1-\nu_s)}{3(2-\nu_s)}\right)$$
$$=$$
$$2\dddot{E}_{xz}\left[\frac{8a_1\eta_1^{\text{int}}(1-\nu_s)}{3\pi(2-\nu_s)\mu_s}\frac{8a_2\eta_2^{\text{int}}(1-\nu_s)}{3\pi(2-\nu_s)\mu_s}\frac{8a_3\eta_3^{\text{int}}(1-\nu_s)}{3\pi(2-\nu_s)\mu_s}\right]+2\ddot{E}_{xz}\left[\frac{8a_1\eta_1^{\text{int}}(1-\nu_s)}{3\pi(2-\nu_s)\mu_s}\frac{8a_2\eta_2^{\text{int}}(1-\nu_s)}{3\pi(2-\nu_s)\mu_s}+\frac{8a_2\eta_2^{\text{int}}(1-\nu_s)}{3\pi(2-\nu_s)\mu_s}\frac{8a_3\eta_3^{\text{int}}(1-\nu_s)}{3\pi(2-\nu_s)\mu_s}\right.$$
$$\left.+\frac{8a_1\eta_1^{\text{int}}(1-\nu_s)}{3\pi(2-\nu_s)\mu_s}\frac{8a_3\eta_3^{\text{int}}(1-\nu_s)}{3\pi(2-\nu_s)\mu_s}\right]+2\dot{E}_{xz}\left[\frac{8a_1\eta_1^{\text{int}}(1-\nu_s)}{3\pi(2-\nu_s)\mu_s}+\frac{8a_2\eta_2^{\text{int}}(1-\nu_s)}{3\pi(2-\nu_s)\mu_s}+\frac{8a_3\eta_3^{\text{int}}(1-\nu_s)}{3\pi(2-\nu_s)\mu_s}\right]+2E_{xz} \tag{56}$$

The general structure of constitutive Σ_{xz}-E_{xz} relations for a matrix-inclusion composite containing N interface phases can be identified from comparing the Σ_{xz}-E_{xz} relations of one, two, and three interface phases, respectively, see Eqs. (43), (55), and (56). Accordingly, it appears that the first-order derivative of the strain, $2\dot{E}_{xz}$, is always multiplied with the sum over all expressions of the form $8a_i\eta_i^{\text{int}}(1-\nu_s)/[3\pi(2-\nu_s)\mu_s]$, with $i=1,2,\ldots,N$. The second-order derivative of the strain, $2\ddot{E}_{xz}$, is always multiplied with the sum over all possible products of two different characteristic times. The third-order derivative of the strain, $2\dddot{E}_{xz}$, is always multiplied with the sum over all possible products of three different characteristic times. This clarifies the general structure: the nth-order derivative of the strain is multiplied with the sum over all possible products of n different characteristic times. The coefficients multiplied with the stress and stress derivatives are just slightly more complex: The stress, Σ_{xz}, is always multiplied with a coefficient being equal to $1/\mu_s$ plus the sum over all expressions $16d_i(1-\nu_s)/[\mu_s 3(2-\nu_s)]$ with $i=1,2,\ldots,N$. The first-order derivative of the stress, $\dot{\Sigma}_{xz}$, is always multiplied with the sum over all the products of characteristic times, $8a_i\eta_i^{\text{int}}(1-\nu_s)/[3\pi(2-\nu_s)\mu_s]$, and corresponding constants being equal to $1/\mu_s$ plus the sum over all expressions $16d_j(1-\nu_s)/[\mu_s 3(2-\nu_s)]$, with $j=1,2,\ldots,N$, minus $16d_i(1-\nu_s)/[\mu_s 3(2-\nu_s)]$. The second-order derivative of the stress, $\ddot{\Sigma}_{xz}$, is always multiplied with the sum over all possible products of two different characteristic times, $8^2a_i\eta_i^{\text{int}}a_j\eta_j^{\text{int}}(1-\nu_s)^2/[3\pi(2-\nu_s)\mu_s]^2$, whereby $i\neq j$, and corresponding constants being equal to $1/\mu_s$ plus the sum over all expressions $16d_k(1-\nu_s)/[\mu_s 3(2-\nu_s)]$, with $k=1,2,\ldots,N$, minus $16(d_i+d_j)(1-\nu_s)/[\mu_s 3(2-\nu_s)]$. The third-order derivative of the stress, $\dddot{\Sigma}_{xz}$, is always multiplied with the sum over all possible products of three different characteristic times, $8^3a_i\eta_i^{\text{int}}a_j\eta_j^{\text{int}}a_k\eta_k^{\text{int}}(1-\nu_s)^3/[3\pi(2-\nu_s)]^3$, whereby $i\neq j$, $i\neq k$, $j\neq k$, and corresponding constants which are equal to $1/\mu_s$ plus the sum over all expressions $16d_l(1-\nu_s)/[\mu_s 3(2-\nu_s)]$, with $l=1,2,\ldots,N$, minus $16(d_i+d_j+d_k)(1-\nu_s)/[\mu_s 3(2-\nu_s)]$. This clarifies the general structure: the nth-order derivative of the stress is multiplied with the sum over all possible products of n different characteristic times and constants being equal to the sum over $1/\mu_s$ plus the sum over all expressions $16d_j(1-\nu_s)/[\mu_s 3(2-\nu_s)]$, with $j=1,2,\ldots,N$, minus all expressions $16d_l(1-\nu_s)/[\mu_s 3(2-\nu_s)]$ with indexes l running over all those values which show up in the products of the characteristic times. In conclusion, mathematical forms of the general Σ_{xz}-E_{xz} relation for a matrix-inclusion composite with N interface phases reads as

$$\left(\frac{1}{\mu_s}+\sum_{l=1}^{N}\frac{1}{\mu_s}\frac{16d_l(1-\nu_s)}{3(2-\nu_s)}\right)\Sigma_{xz}+\sum_{n=1}^{N}\left(\sum_{i_1=1}^{N-n+1}\cdots\left(\sum_{i_a=i_{a-1}+1}^{N-(n-a)+1}\cdots\left(\sum_{i_n=i_{n-1}+1}^{N}\left(\left(\left(\frac{1}{\mu_s}+\sum_{l=1}^{N}\frac{1}{\mu_s}\frac{16d_l(1-\nu_s)}{3(2-\nu_s)}\right)\right.\right.\right.\right.$$
$$\left.\left.\left.\left.-\sum_{j\in\{i_1,\ldots,i_n\}}\frac{1}{\mu_s}\frac{16d_j(1-\nu_s)}{3(2-\nu_s)}\right)\left(\prod_{k\in\{i_1,\ldots,i_n\}}\frac{8a_k\eta_k^{\text{int}}(1-\nu_s)}{3\pi(2-\nu_s)\mu_s}\right)\right)\right)\cdots\right)\cdots\right)\frac{\partial^n\Sigma_{xz}}{\partial t^n}$$
$$=$$
$$2E_{xz}+\sum_{n=1}^{N}\left(\sum_{i_1=1}^{N-n+1}\cdots\left(\sum_{i_a=i_{a-1}+1}^{N-(n-a)+1}\cdots\left(\sum_{i_n=i_{n-1}+1}^{N}\left(\prod_{j\in\{i_1,\ldots,i_n\}}\frac{8a_j\eta_j^{\text{int}}(1-\nu_s)}{3\pi(2-\nu_s)\mu_s}\right)\right)\cdots\right)\cdots\right)\frac{\partial^n 2E_{xz}}{\partial t^n} \tag{57}$$

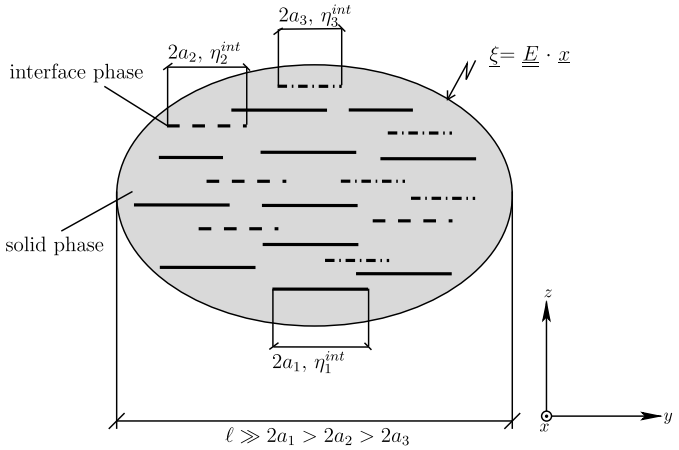

Fig. 9. Matrix-interface composite with three families of 2D flat, parallel, spherical interfaces; 2D sketch of 3D representative volume elements

Interface Micromechanics Assessment of Rheological Models

Here, we establish relations between the Kelvin-Voigt chain-related and the Maxwell chain-related spring and dashpot parameters, as well as between these parameters and the micromechanics-related quantities of the matrix-interface composites, namely the shear modulus and Poisson's ratio of the solid matrix, as well as the sizes, viscosities, and densities of the embedded 2D interfaces. To this end, we compare the Kelvin-Voigt chain-related, Maxwell chain-related, and micromechanics-related coefficients occurring in the differential equations comprising stresses, strains, and their temporal derivatives; see Eqs. (20), (37), and (57), and consider $\tau = \Sigma_{xz}$ as well as $\gamma = 2E_{xz}$.

Relations between Kelvin Voigt Chain Parameters and Micromechanical Quantities

Links between spring stiffnesses and damper viscosities of Kelvin Voigt chains, on the one hand, and micromechanical properties, on the other hand, are obtained from comparing the coefficients appearing in the two Nth-order differential equations, Eqs. (20) and (57). This leads to the identity

$$\left(\frac{1}{\mu_e}+\sum_{l=1}^{N}\frac{1}{\mu_l}\right)=\left(\frac{1}{\mu_s}+\sum_{l=1}^{N}\frac{1}{\mu_s}\frac{16d_l(1-\nu_s)}{3(2-\nu_s)}\right) \tag{58}$$

as well as to

$$\sum_{n=1}^{N}\left(\sum_{i_1=1}^{N-n+1}\cdots\left(\sum_{i_a=i_{a-1}+1}^{N-(n-a)+1}\cdots\left(\sum_{i_n=i_{n-1}+1}^{N}\left(\left(\left(\frac{1}{\mu_e}+\sum_{l=1}^{N}\frac{1}{\mu_l}\right)-\sum_{j\in\{i_1,\ldots,i_n\}}\frac{1}{\mu_j}\right)\left(\prod_{k\in\{i_1,\ldots,i_n\}}\frac{\eta_k}{\mu_k}\right)\right)\right)\cdots\right)\cdots\right)$$
$$=$$
$$\sum_{n=1}^{N}\left(\sum_{i_1=1}^{N-n+1}\cdots\left(\sum_{i_a=i_{a-1}+1}^{N-(n-a)+1}\cdots\left(\sum_{i_n=i_{n-1}+1}^{N}\left(\left(\left(\frac{1}{\mu_s}+\sum_{l=1}^{N}\frac{1}{\mu_s}\frac{16d_l(1-\nu_s)}{3(2-\nu_s)}\right)-\sum_{j\in\{i_1,\ldots,i_n\}}\frac{1}{\mu_s}\frac{16d_j(1-\nu_s)}{3(2-\nu_s)}\right)\left(\prod_{k\in\{i_1,\ldots,i_n\}}\frac{8a_k\eta_k^{\text{int}}(1-\nu_s)}{3\pi(2-\nu_s)\mu_s}\right)\right)\right)\cdots\right)\cdots\right) \tag{59}$$

and finally to

$$\sum_{n=1}^{N}\left(\sum_{i_1=1}^{N-n+1}\cdots\left(\sum_{i_a=i_{a-1}+1}^{N-(n-a)+1}\cdots\left(\sum_{i_n=i_{n-1}+1}^{N}\left(\prod_{j\in\{i_1,\ldots,i_n\}}\frac{\eta_j}{\mu_j}\right)\right)\cdots\right)\cdots\right)$$
$$=\sum_{n=1}^{N}\left(\sum_{i_1=1}^{N-n+1}\cdots\left(\sum_{i_a=i_{a-1}+1}^{N-(n-a)+1}\cdots\left(\sum_{i_n=i_{n-1}+1}^{N}\left(\prod_{j\in\{i_1,\ldots,i_n\}}\frac{8a_j\eta_j^{\text{int}}(1-\nu_s)}{3\pi(2-\nu_s)\mu_s}\right)\right)\cdots\right)\cdots\right) \tag{60}$$

Eqs. (58), (59), and (60) represent $2N+1$ algebraic equations, with the following solutions:

$$\mu_e=\mu_s,\qquad \left.\begin{aligned}\mu_i&=\frac{3\mu_s(2-\nu_s)}{16d_i(1-\nu_s)}\\ \eta_i&=\frac{a_i\eta_i^{\text{int}}}{2\pi d_i}\end{aligned}\right\}\quad i=1,2,\ldots,N \tag{61}$$

see also Table 1. We observe that Eq. (61) is formally identical to the relations derived for the special case $N=1$ in the companion paper, see (Shahidi et al. 2015b).

Relations between Maxwell Chain Parameters and Viscosities as Well as Micromechanical Quantities

Links between spring stiffnesses and damper viscosities of Maxwell chains, on the one hand, and micromechanical properties, on the other hand, are obtained from comparing the coefficients appearing in the two Nth-order differential equations, Eqs. (37) and (57). This leads to the identity

$$\frac{1}{\mu_E}=\left(\frac{1}{\mu_s}+\sum_{l=1}^{N}\frac{1}{\mu_s}\frac{16d_l(1-\nu_s)}{3(2-\nu_s)}\right) \tag{62}$$

as well as to

$$\frac{1}{\mu_E}\sum_{n=I}^{N}\left(\sum_{i_I=I}^{N-n+I}\cdots\left(\sum_{i_a=i_{a-I}+I}^{N-(n-a)+I}\cdots\left(\sum_{i_n=i_{n-I}+I}^{N}\left(\prod_{j\in\{i_1,\ldots,i_n\}}\frac{\eta_j}{\mu_j}\right)\right)\cdots\right)\cdots\right)$$

$$=$$

$$\sum_{n=1}^{N}\left(\sum_{i_1=1}^{N-n+1}\cdots\left(\sum_{i_a=i_{a-1}+1}^{N-(n-a)+1}\cdots\left(\sum_{i_n=i_{n-1}+1}^{N}\left(\left(\left(\frac{1}{\mu_s}+\sum_{l=1}^{N}\frac{1}{\mu_s}\frac{16d_l(1-\nu_s)}{3(2-\nu_s)}\right)-\sum_{j\in\{i_1,\ldots,i_n\}}\frac{1}{\mu_s}\frac{16d_j(1-\nu_s)}{3(2-\nu_s)}\right)\left(\prod_{k\in\{i_1,\ldots,i_n\}}\frac{8a_k\eta_k^{\text{int}}(1-\nu_s)}{3\pi(2-\nu_s)\mu_s}\right)\right)\right)\cdots\right)\cdots\right) \tag{63}$$

and finally to

$$\frac{1}{\mu_E}\sum_{n=I}^{N}\left(\sum_{i_I=I}^{N-n+I}\cdots\left(\sum_{i_a=i_{a-I}+I}^{N-(n-a)+I}\cdots\left(\sum_{i_n=i_{n-I}+I}^{N}\left(\left(\mu_E+\sum_{j\in\{i_1,\ldots,i_n\}}\mu_j\right)\left(\prod_{k\in\{i_I,\ldots,i_n\}}\frac{\eta_k}{\mu_k}\right)\right)\right)\cdots\right)\cdots\right)$$

$$=\sum_{n=1}^{N}\left(\sum_{i_1=1}^{N-n+1}\cdots\left(\sum_{i_a=i_{a-1}+1}^{N-(n-a)+1}\cdots\left(\sum_{i_n=i_{n-1}+1}^{N}\left(\prod_{j\in\{i_1,\ldots,i_n\}}\frac{8a_j\eta_j^{\text{int}}(1-\nu_s)}{3\pi(2-\nu_s)\mu_s}\right)\right)\cdots\right)\cdots\right) \tag{64}$$

Eqs. (62)–(64) represent a system of $2N+1$ non-linear, coupled algebraic equations. The analytical solution for $N=1$ is presented in the companion paper, see Table 1 in (Shahidi et al. 2015b), but already for $N=2$, analytical solutions involve complicated terms involving square root–expressions, for $N=3$ cubic roots are found, and so on. We conclude that for the general situation of N interface phases and N Maxwell chains, Eqs. (62)–(64) have to be solved numerically.

The counterintuitive nature of Maxwell chains very clearly manifests itself already when discussing the expectedly simple relations between two interface families and two rheological units, respectively. Surprisingly, not only both dashpot viscosities η_I and η_{II} but also both spring stiffnesses μ_I and μ_{II} depend in a non-trivial fashion on the properties of both interface families and on the properties of the matrix, i.e.,

$$\begin{aligned}\eta_I &= \eta_I(d_1,a_1,\eta_1^{\text{int}};d_2,a_2,\eta_2^{\text{int}};\mu_s,\nu_s)\\ \eta_{II} &= \eta_{II}(d_1,a_1,\eta_1^{\text{int}};d_2,a_2,\eta_2^{\text{int}};\mu_s,\nu_s)\\ \mu_I &= \eta_I(d_1,a_1,\eta_1^{\text{int}};d_2,a_2,\eta_2^{\text{int}};\mu_s,\nu_s)\\ \mu_{II} &= \eta_{II}(d_1,a_1,\eta_1^{\text{int}};d_2,a_2,\eta_2^{\text{int}};\mu_s,\nu_s)\end{aligned} \tag{65}$$

Analytical closed-form solutions contain lengthy square-root expressions and are so expanded that they go beyond the scope of this paper. Anyway, already Eqs. (65) underline that it is impossible to associate individual Maxwell units with only one corresponding interface family. Instead, Eqs. (65) clarify that each Maxwell unit depends on *all* interface families, and this results from the non-linearities of the system of Eqs. (62)–(64). Particularly, the Maxwell spring stiffnesses μ_I and μ_{II} do not only depend on the elastic properties of the solid matrix and on the interface sizes, but also on the viscous properties of the interfaces. This prohibits any meaningful graphical illustration of these stiffnesses as functions of the matrix stiffness and the interface densities. Merely the

Table 1. Relations between Spring Stiffnesses and Dashpot Viscosities of a Kelvin-Voigt Chain with N Units, and Micromechanical Quantities of a Matrix-Interface Composite with N Interface Families, $i=1,2,3,\ldots,N$

Models	Micromechanics according to Fig. 7
Kelvin-Voigt chain according to Fig. 1	$\mu_e=\mu_s\ \mu_i=\dfrac{3\mu_s(2-\nu_s)}{16d_i(1-\nu_s)}\ \eta_i=\dfrac{a_i\eta_i^{\text{int}}}{2\pi d_i}$

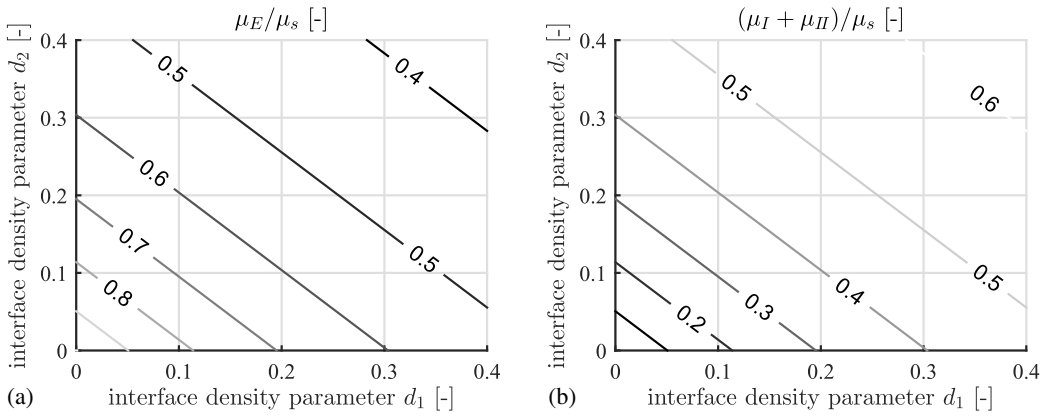

Fig. 10. Dimensionless spring stiffnesses of Maxwell representation with $N=2$, as functions of dimensionless interface density parameters d_1 and d_2: (a) μ_E/μ_s, and (b) $(\mu_I+\mu_{II})/\mu_s$

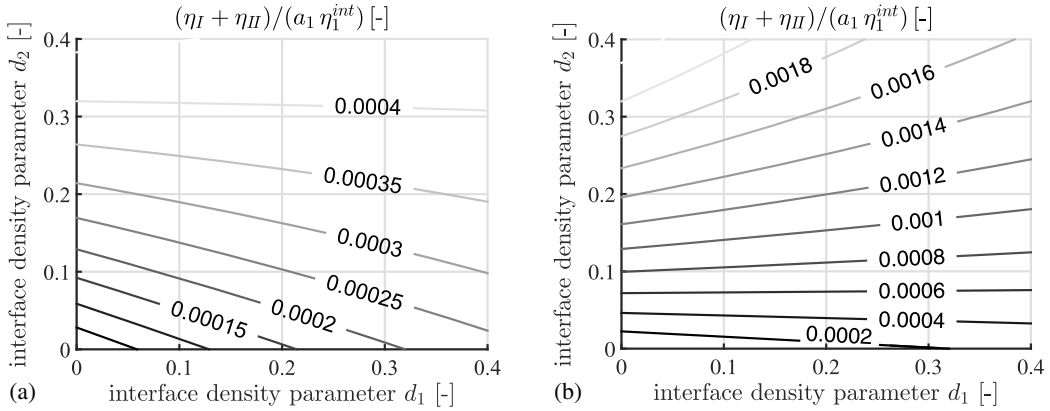

Fig. 11. Dimensionless sum of dashpot viscosities of Maxwell representation with $N = 2$ and $\nu_s = 0.27$, as function of dimensionless interface density parameters d_1 and d_2: $(\eta_I + \eta_{II})/(a_1\eta_1^{\text{int}})$ (a) for $(a_2\eta_2^{\text{int}})/(a_1\eta_1^{\text{int}}) = 2$, and (b) for $(a_2\eta_2^{\text{int}})/(a_1\eta_1^{\text{int}}) = 10$

sum of the two spring stiffnesses, μ_I and μ_{II}, is independent of the viscous properties of the two interface families, and reads as

$$\mu_I + \mu_{II} = \frac{16\mu_s(d_1 + d_2)(1 - \nu_s)}{3(2 - \nu_s) + 16(d_1 + d_2)(1 - \nu_s)} \tag{66}$$

This allows for the sought graphical illustration; see Fig. 10. Notably, the sum $\mu_I + \mu_{II}$ has a clear mechanical meaning, because it quantifies the time-dependent loss of apparent stiffness in a creep test or in a relaxation test, respectively. Also the sum of the two dashpot viscosities allows for a compact closed-form solution (Fig. 11)

$$\eta_I + \eta_{II} = \frac{128(1 - \nu_s)^2(a_1\eta_1^{\text{int}}d_1 + a_2\eta_2^{\text{int}}d_2)}{\pi[3(2 - \nu_s) + 16(d_1 + d_2)(1 - \nu_s)]^2} \tag{67}$$

Conclusions

Both Kelvin-Voigt and Maxwell chain models consisting of N chain elements are well suited to describe the time-dependent behavior of matrix-interface composites with N different interface families, exhibiting different sizes and viscosities. Still, the chosen type of the rheological representation matters significantly when it comes to the mathematical complexity of the relations between the microstructural quantities of matrix-interface composites and the rheological parameters such as spring stiffnesses and dashpot viscosities. As for Kelvin-Voigt chain models, the "intuitive" relations identified for one interface family and one Kelvin-Voigt unit—see the companion paper (Shahidi et al. 2015b)—are conceptually identical with the relations found for N interface families and N Kelvin-Voigt units; see Eqs. (58)–(61). As for Maxwell chain models, however, the mathematical complexity of the relations increases with increasing number of interface families and number of Maxwell units; see Eqs. (62)–(64). In other words, from the viewpoint of interface micromechanics, Kelvin-Voigt chain models are conceptually preferable to the (fully equivalent) Maxwell chain models.

Kelvin-Voigt representations also shed light on a particularly interesting aspect of interface interaction: Although the micromechanical relationship of Eq. (42) shows that the average dislocation related to one family of interfaces depends on the tractions encountered in this as well as in all other interface families, the parameters of each Kelvin-Voigt unit depend solely on the parameters characterizing a single family of interfaces, according to Eq. (61). This might lead someone to the idea that the Kelvin-Voigt representation would not consider anymore the mutual interface interactions. However, looking more closely at the problem, the Kelvin-Voigt representation actually evidences that mutual interaction of the chain elements (and hence of the interface families) is only prohibited in the case where the stresses are prescribed: then one and the same stress τ is carried by each and every chain element. However, under prescribed (i.e., constant, non-zero) strain γ, the evolving stress does indeed depend on the interaction of all chain elements (and hence, on the interaction among all interface families). Hence, the Kelvin-Voigt representation turns out as a particularly straightforward tool to explain the interaction of interface families under prescribed overall stress and strain, respectively. The same argument can be developed on the basis of purely micromechanical considerations, as given in full detail in (Shahidi et al. 2015a): The overall macroscopic stress subjected to an RVE made up of an elastic matrix hosting non-elastic 2D interfaces is identical to the average of the microscopic matrix stresses, whereas the macroscopic strains are the sum of the average microscopic matrix strains (being related to the microscopic stresses by the elastic properties of the solid matrix) and a strain-like contribution from the average interface dislocations. Hence, if macroscopic stresses are prescribed, the dislocation evolution is solely driven by the boundary of the RVE (through macroscopic properties), thereby prohibiting any interface interaction which would be independent of the macroscopically prescribed stress and strain states. The situation changes with prescribed macroscopic strain which does not imply any restrictions on the microscopic strains and stresses, and therefore allows for evolving interactions between the interfaces, driven by their geometric as well as viscous properties.

Moreover, according to our results relating rheological parameters of chain models to interface properties, the need of introducing Maxwell or Kelvin-Voigt chains for the representation of complex creep behavior would indicate the existence of microscopic interface size distributions. Different sizes of interfaces, located at the microstructure of a creeping material, namely, manifest themselves at the macroscale of the materials as different characteristic creep times. In other words, interface micromechanics suggests that continuous (or discrete) interface size distributions lead to continuous (or discrete) spectra of macroscopic characteristic creep times. Such spectra have been often used in the context of modeling aging or non-aging creep of concrete, based on either Maxwell or Kelvin-Voigt chain representations (see, e.g., Bažant 1977; Bažant and Xi 1995; Bažant and Huet 1999). In the aging

case, spring and dashpot parameters standardly evolve in time, and the presented micromechanical assessment of rheological chain models then obviously proposes that the maturation of concrete might express itself in temporal changes in interface size and density. Thereby, interface sizes range from several nanometers in elementary clusters of calcium-silicate-hydrates, C-S-H, (Pellenq et al. 2009), to tens or hundreds of micrometers, as expected throughout the polydisperse features of cement hydration products (Masoero et al. 2012; Thomas et al. 2011). On the other hand, the relation between characteristic times and interface size proposes ever increasing interface sizes under local mechanical load (interface spreading, a phenomenon close to what is normally called crack propagation) as a probable reason for logarithmic (or power-law type) creep, both at the microscale (Vandamme and Ulm 2009, 2013) and at the macroscale (Bažant et al. 2012). From a more quantitative viewpoint, it appears appealing to invest into upscaling the fundamental interface blocks investigated in the present contribution, to clusters involving interfaces oriented in all space directions, representing typical hydrate phases as used in multiscale micromechanics models which have been recently developed for predicting the macroscopic creep of concrete from the composition and the hydration degree of the material (Scheiner and Hellmich 2009; Sanahuja and Toulemonde 2011; Sanahuja and Dormieux 2010; Tran et al. 2013). Investigation of such hydrated creep-active phases extends obviously beyond concrete mechanics, with clay (Dormieux et al. 2006) and bone (Eberhardsteiner et al. 2014) as particularly prominent other material systems of great fundamental and technological interest. In this context, it will be desirable to gain access to physical values of interface viscosities, in order to develop predictive multiscale creep models for hydrated materials such as hydroxyapatite in bone and biomimetic materials. Given that viscous interfaces are expected on diameter length scales as small as some hundreds of nanometers up to a few micrometers, and of thicknesses which may even be below 1 nanometer, together with technological difficulties to perform "microshear tests" at such microscales, molecular dynamics simulation (Pellenq et al. 2009; Youssef et al. 2011; Dubey and Tomar 2009; Qu and Tomar 2014) appears to be an interesting candidate for direct interface viscosity identification; in addition to downscaled viscosity values from various independent macroscopic tests, as done, e.g., in (Eberhardsteiner et al. 2014).

Appendix. Expanded Versions of Stress-Strain Relations

Expanded Version of Generalized Kelvin-Voigt Model

Eq. (20) can be understood easier in the expanded form as

$$\gamma+\left(\sum_{i=1}^{N}\frac{\eta_i}{\mu_i}\right)\frac{\partial\gamma}{\partial t}+\left(\sum_{i=1}^{N-1}\left(\sum_{j=i+1}^{N}\frac{\eta_i}{\mu_i}\frac{\eta_j}{\mu_j}\right)\frac{\partial^2\gamma}{\partial t^2}+\cdots+\left(\sum_{i_1=1}^{N-n+1}\cdots\left(\sum_{i_a=i_{a-1}+1}^{N-(n-a)+1}\cdots\left(\sum_{i_n=i_{n-1}+1}^{N}\left(\prod_{j\in\{i_1,\ldots,i_n\}}\frac{\eta_j}{\mu_j}\right)\right)\cdots\right)\cdots\right)\frac{\partial^n\gamma}{\partial t^n}+\cdots+\left(\prod_{i=1}^{N}\frac{\eta_i}{\mu_i}\right)\frac{\partial^N\gamma}{\partial t^N}$$

$$=$$

$$\left(\frac{1}{\mu_e}+\sum_{l=1}^{N}\frac{1}{\mu_l}\right)\tau+\left(\sum_{i=1}^{N}\left(\left(\frac{1}{\mu_e}+\sum_{l=1}^{N}\frac{1}{\mu_l}\right)-\frac{1}{\mu_i}\right)\frac{\eta_i}{\mu_i}\right)\frac{\partial\tau}{\partial t}+\left(\sum_{i=1}^{N-1}\left(\sum_{j=i+1}^{N}\left(\left(\frac{1}{\mu_e}+\sum_{l=1}^{N}\frac{1}{\mu_l}\right)-\frac{1}{\mu_i}-\frac{1}{\mu_j}\right)\frac{\eta_i}{\mu_i}\frac{\eta_j}{\mu_j}\right)\right)\frac{\partial^2\tau}{\partial t^2}+\cdots+$$

$$\left(\sum_{i_1=1}^{N-n+1}\cdots\left(\sum_{i_a=i_{a-1}+1}^{N-(n-a)+1}\cdots\left(\sum_{i_n=i_{n-1}+1}^{N}\left(\left(\left(\frac{1}{\mu_e}+\sum_{l=1}^{N}\frac{1}{\mu_l}\right)-\sum_{j\in\{i_1,\ldots,i_n\}}\frac{1}{\mu_j}\right)\left(\prod_{k\in\{i_1,\ldots,i_n\}}\frac{\eta_k}{\mu_k}\right)\right)\right)\cdots\right)\cdots\right)\frac{\partial^n\tau}{\partial t^n}+\cdots+\frac{1}{\mu_e}\left(\prod_{i=1}^{N}\frac{\eta_i}{\mu_i}\right)\frac{\partial^N\tau}{\partial t^N} \tag{68}$$

Expanded Version of Generalized Maxwell Model

Eq. (37) can be understood easier in the expanded form as

$$\tau+\left(\sum_{i=1}^{N}\frac{\eta_i}{\mu_i}\right)\frac{\partial\tau}{\partial t}+\left(\sum_{i=1}^{N-1}\left(\sum_{j=i+1}^{N}\frac{\eta_i}{\mu_i}\frac{\eta_j}{\mu_j}\right)\frac{\partial^2\tau}{\partial t^2}+\cdots+\left(\sum_{i_1=1}^{N-n+1}\cdots\left(\sum_{i_a=i_{a-1}+1}^{N-(n-a)+1}\cdots\left(\sum_{i_n=i_{n-1}+1}^{N}\left(\prod_{j\in\{i_1,\ldots,i_n\}}\frac{\eta_j}{\mu_j}\right)\right)\cdots\right)\cdots\right)\frac{\partial^n\tau}{\partial t^n}+\cdots+\left(\prod_{i=1}^{N}\frac{\eta_i}{\mu_i}\right)\frac{\partial^N\tau}{\partial t^N}$$

$$=$$

$$\mu_E\gamma+\left(\sum_{i=1}^{N}(\mu_E+\mu_i)\frac{\eta_i}{\mu_i}\right)\frac{\partial\gamma}{\partial t}+\left(\sum_{i=1}^{N-1}\left(\sum_{j=i+1}^{N}(\mu_E+\mu_i+\mu_j)\frac{\eta_i}{\mu_i}\frac{\eta_j}{\mu_j}\right)\right)\frac{\partial^2\gamma}{\partial t^2}+\cdots+$$

$$\left(\sum_{i_1=1}^{N-n+1}\cdots\left(\sum_{i_a=i_{a-1}+1}^{N-(n-a)+1}\cdots\left(\sum_{i_n=i_{n-1}+1}^{N}\left(\left(\mu_E+\sum_{j\in\{i_1,\ldots,i_n\}}\mu_j\right)\left(\prod_{k\in\{i_1,\ldots,i_n\}}\frac{\eta_k}{\mu_k}\right)\right)\right)\cdots\right)\cdots\right)\frac{\partial^n\gamma}{\partial t^n}+\cdots+\left(\mu_E+\sum_{j=1}^{N}\mu_j\right)\left(\prod_{i=1}^{N}\frac{\eta_i}{\mu_i}\right)\frac{\partial^N\gamma}{\partial t^N} \tag{69}$$

Relation between Parameters Characterizing Kelvin-Voigt and Maxwell Chains, Respectively

The link between the spring and dashpot constants of the Kelvin-Voigt chain model and of the Maxwell chain model can be expressed as

$$\frac{1}{\mu_E} = \left(\frac{1}{\mu_e} + \sum_{l=1}^{N} \frac{1}{\mu_l}\right) \tag{70}$$

as well as

$$\frac{1}{\mu_E}\sum_{n=I}^{N}\left(\sum_{i_I=I}^{N-n+I} \cdots \left(\sum_{i_a=i_{a-I}+I}^{N-(n-a)+I} \cdots \left(\sum_{i_n=i_{n-I}+I}^{N}\left(\prod_{j\in\{i_I,\ldots,i_n\}}\frac{\eta_j}{\mu_j}\right)\right)\cdots\right)\cdots\right)$$
$$=$$
$$\sum_{n=1}^{N}\left(\sum_{i_1=1}^{N-n+1} \cdots \left(\sum_{i_a=i_{a-1}+1}^{N-(n-a)+1} \cdots \left(\sum_{i_n=i_{n-1}+1}^{N}\left(\left(\left(\frac{1}{\mu_e}+\sum_{l=1}^{N}\frac{1}{\mu_l}\right) - \sum_{j\in\{i_1,\ldots,i_n\}}\frac{1}{\mu_j}\right)\right.\right.\right.$$
$$\left.\left.\left.\times\left(\prod_{k\in\{i_1,\ldots,i_n\}}\frac{\eta_k}{\mu_k}\right)\right)\right)\cdots\right)\cdots\right) \tag{71}$$

and

$$\frac{1}{\mu_E}\sum_{n=I}^{N}\left(\sum_{i_I=I}^{N-n+I} \cdots \left(\sum_{i_a=i_{a-I}+I}^{N-(n-a)+I} \cdots \left(\sum_{i_n=i_{n-I}+I}^{N}\left(\left(\mu_E + \sum_{j\in\{i_I,\ldots,i_n\}}\mu_j\right)\left(\prod_{k\in\{i_I,\ldots,i_n\}}\frac{\eta_k}{\mu_k}\right)\right)\right)\cdots\right)\cdots\right)$$
$$=$$
$$\sum_{n=1}^{N}\left(\sum_{i_1=1}^{N-n+1} \cdots \left(\sum_{i_a=i_{a-1}+1}^{N-(n-a)+1} \cdots \left(\sum_{i_n=i_{n-1}+1}^{N}\left(\prod_{j\in\{i_I,\ldots,i_n\}}\frac{\eta_j}{\mu_j}\right)\right)\cdots\right)\cdots\right) \tag{72}$$

Notation

The following symbols are used in this paper:

$\underline{\underline{\underline{A}}}_i$ = third-order concentration tensor of the ith interface family, $i = 1,2,\ldots,N$;
a = index in the stress-strain relations given by Eqs. (20), (37), (57), (59), (60), (63), (64), (68), (69), (71), and (72);
a_i = radius of the ith interface family, $i = 1,2,\ldots,N$;
$\underline{\underline{\underline{B}}}_i$ = third-order Biot-type influence tensor of the ith interface family, $i = 1,2,\ldots,N$;
$\underline{\underline{\underline{C}}}_s$ = fourth-order stiffness tensor of solid;
$\underline{\underline{\underline{C}}}_s^{-1}$ = inverse of fourth-order stiffness tensor of solid;
$\underline{\underline{\underline{C}}}_{\text{hom}}$ = fourth-order homogenized stiffness tensor of matrix-interface composite;
$\underline{\underline{D}}_{ij}$ = second-order influence tensor linking interface families i and j;
d_i = interface density parameter of the ith interface family, $i = 1,2,\ldots,N$;
$\underline{\underline{E}}$ = second-order tensor of macroscopic strain;
E_{xz} = shear component of macroscopic strain;
$\underline{e}_x$, $\underline{e}_y$, $\underline{e}_z$ = unit base vectors of Cartesian coordinate system;
$\underline{\underline{\underline{I}}}$ = symmetric fourth-order identity tensor;
$\underline{\underline{\underline{I}}}_{\text{dev}}$ = deviatoric part of $\underline{\underline{\underline{I}}}$;
$\underline{\underline{\underline{I}}}_{\text{vol}}$ = volumetric part of $\underline{\underline{\underline{I}}}$;
k_s = bulk modulus of solid phase;
ℓ = characteristic size of RVE;
N = number of Maxwell or Kelvin-Voigt units;
RVE = Representative volume element;
s = index for solid phase;
$\underline{T}$ = interface traction vector;
$T_{i,x}$ = shear component of traction vector in the ith interface family;
x, y, z = Cartesian coordinates;
$\underline{x}$ = position vector;
γ = shear strain;
γ_e = shear strain of additional elastic spring of Kelvin-Voigt chain;
γ_E = shear strain of additional elastic spring of Maxwell chain;
γ_h = solution for homogeneous differential equation for γ;
γ_i = shear strain of ith rheological unit; Kelvin-Voigt chain: $i = 1,2,\ldots,N$; Maxwell chain: $i = I, II, \ldots, N$;
γ_i^{μ} = shear strain of spring of ith rheological unit in Maxwell chain: $i = I, II, \ldots, N$;
γ_i^{η} = shear strain of dashpot of ith rheological unit in Maxwell chain: $i = I, II, \ldots, N$;
γ_p = particulate integral γ;
δ = Kronecker delta;
$\underline{\underline{\varepsilon}}$ = second-order tensor of microscopic linear strain;
η_i^{int} = viscosity of the ith interface family, $i = 1,2,\ldots,N$;
η_i = viscosity constant of dashpot in the ith rheological unit; Kelvin-Voigt chain $i = 1,2,\ldots,N$; Maxwell chain, $i = I, II, \ldots, N$;

μ_e = stiffness of additional elastic spring of Kelvin-Voigt chain;
μ_E = stiffness of additional elastic spring of Maxwell chain;
μ_i = stiffness of spring in the ith rheological unit; Kelvin-Voigt chain $i = 1,2,\ldots,N$; Maxwell chain, $i = I, II, \ldots, N$;
μ_s = shear modulus of isotropic solid matrix;
ν_s = Poisson's ratio of isotropic solid matrix;
$\underline{\xi}$ = displacement vector;
$[\![\xi]\!]_{i,x}$ = shear component of dislocation of interfaces in shear direction;
$\underline{\underline{\sigma}}$ = second-order tensor of microscopic stress;
$\underline{\underline{\Sigma}}$ = macroscopic stress;
Σ_{xz} = shear component of macroscopic stress;
τ = shear stress;
τ_e = shear stress of additional elastic spring of Kelvin-Voigt chain;
τ_E = shear stress of additional elastic spring of Maxwell chain;
τ_h = solution for homogeneous differential equation for shear stress;
τ_i = shear stress of ith rheological unit; Kelvin-Voigt chain $i = 1,2,\ldots,N$; Maxwell chain $i = I, II, \ldots, N$;
τ_i^{μ} = shear stress of spring of ith rheological unit in Kelvin-Voigt chain: $i = 1,2,\ldots,N$;
τ_i^{η} = shear stress of dashpot of ith rheological unit in Kelvin-Voigt chain: $i = 1,2,\ldots,N$;
τ_p = particulate integral for shear stress;
∂ = partial derivative;
: = second-order tensor contraction;
$\dot{\bullet}$ = partial derivative with respect to time ("rate") of quantity "$\bullet$";
$\ddot{\bullet}$ = second partial derivative with respect to time of quantity "$\bullet$";
$\dddot{\bullet}$ = third partial derivative with respect to time of quantity "$\bullet$"; and
$\otimes$ = dyadic product.

References

Bažant, Z. (1977). "Thermodynamics of solidifying or melting viscoelastic material." *J. Eng. Mech. Div.*, 105(6), 933–952.

Bažant, Z. P., Hauggaard, A. B., Baweja, S., Ulm, F.-J. (1997). "Microprestress-solidification theory for concrete creep. I: Aging and drying effects." *J. Eng. Mech.*, 10.1061/(ASCE)0733-9399(1997)123:11(1188), 1188–1194.

Bažant, Z. P., and Huet, C. (1999). "Thermodynamic functions for ageing viscoelasticity: Integral form without internal variables." *Int. J. Solids Struct.*, 36(26), 3993–4016.

Bažant, Z. P., and Xi, Y. (1995). "Continuous retardation spectrum for solidification theory of concrete creep." *J. Eng. Mech.*, 10.1061/(ASCE)0733-9399(1995)121:2(281), 281–288.

Bažant, Z. P., Yu, Q., and Li, G. (2012). "Excessive long-time deflections of prestressed box girders. I: Record-span bridge in Palau and other paradigms." *J. Struct. Eng.*, 10.1061/(ASCE)ST.1943-541X.0000487, 676–686.

Dormieux, L., Lemarchand, E., and Sanahuja, J. (2006). "Macroscopic behavior of porous materials with lamellar microstructure." *Comptes Rendus—Mecanique*, 334(5), 304–310.

Dubey, D. K., and Tomar, V. (2009). "Understanding the influence of structural hierarchy and its coupling with chemical environment on the strength of idealized tropocollagen-hydroxyapatite biomaterials." *J. Mech. Phys. Solids*, 57(10), 1702–1717.

Eberhardsteiner, L., Hellmich, C., and Scheiner, S. (2014). "Layered water in crystal interfaces as source for bone viscoelasticity: Arguments from a multiscale approach." *Comput. Methods Biomech. Biomed. Eng.*, 17(1), 48–63.

Kelley, B. S., Lafferty, J. F., Bowman, D. A., and Clark, P. A. (1983). "Rhesus monkey intervertebral disk viscoelastic response to shear stress." *J. Biomech. Eng.*, 105(1), 51–54.

Liu, H., Polak, M. A., and Penlidis, A. (2008). "A practical approach to modeling time-dependent nonlinear creep behavior of polyethylene for structural applications." *Polym. Eng. Sci.*, 48(1), 159–167.

Masoero, E., Del Gado, E., Pellenq, R. J.-M., Ulm, F.-J., and Yip, S. (2012). "Nanostructure and nanomechanics of cement: Polydisperse colloidal packing." *Phys. Rev. Lett.*, 109(15), 155503(1)–155503(4).

Maxwell, J. C. (1867). "On the dynamic theory of gases." *Philos. Trans. R. Soc. London*, 157(Jan), 49–88.

Meyer, O. E. (1878). "Ueber die elastische Nachwirkung [Concerning elastic after effects]." *Ann. Physik u. Chemie*, 240(6), 249–267 (in German).

Pellenq et al. (2009). "A realistic molecular model of cement hydrates." *Proc. Natl. Acad. Sci. U.S.A.*, 106(38), 16102–16107.

Qu, T., and Tomar, V. (2014). "An analysis of the effects of temperature and structural arrangements on the thermal conductivity and thermal diffusivity of tropocollagen-hydroxyapatite interfaces." *Mater. Sci. Eng. C*, 38(1), 28–38.

Sanahuja, J., and Dormieux, L. (2010). "Creep of a C-S-H gel: A micromechanical approach." *Anais da Academia Brasileira de Ciencias*, 82(1), 25–41.

Sanahuja, J., and Toulemonde, C. (2011). "Numerical homogenization of concrete microstructures without explicit meshes." *Cem. Concr. Res.*, 41(12), 1320–1329.

Scheiner, S., and Hellmich, C. (2009). "Continuum microviscoelasticity model for aging basic creep of early-age concrete." *J. Eng. Mech.*, 10.1061/(ASCE)0733-9399(2009)135:4(307), 307–323.

Shahidi, M., Pichler, B., and Hellmich, C. (2014). "Viscous interfaces as source for material creep: A continuum micromechanics approach." *Eur. J. Mech., A/Solids*, 45(May/Jun), 41–58.

Shahidi, M., Pichler, B., and Hellmich, C. (2015a). "How interface size, density, and viscosity affect creep and relaxation functions of matrix-interface composites—A micromechanical study." *Acta Mech.*, 1–24.

Shahidi, M., Pichler, B., and Hellmich, C. (2015b). "Interfacial micromechanics assessment of classical rheological models I: Single interface size and viscosity." *J. Eng. Mech.*, 04015092.

Šmilauer, V., and Bažant, Z. P. (2010). "Identification of viscoelastic C-S-H behavior in mature cement paste by FFT-based homogenization method." *Cem. Concr. Res.*, 40(2), 197–207.

Thomas, J. J., et al. (2011). "Modeling and simulation of cement hydration kinetics and microstructure development." *Cem. Concr. Res.*, 41(12), 1257–1278.

Thomson, W. L. K. (1865). "On the elasticity and viscosity of metals." *Proc. R. Soc. London*, 14, 289–297.

Tran, A. B., Yvonnet, J., He, Q., Toulemonde, C., and Sanahuja, J. (2013). "A four-scale homogenization analysis of creep of a nuclear containment structure." *Nucl. Eng. Des.*, 265, 712–726.

Vandamme, M., and Ulm, F. J. (2009). "Nanogranular origin of concrete creep." *Proc. Natl. Acad. Sci. U.S.A.*, 106(26), 10552–10557.

Vandamme, M., and Ulm, F. J. (2013). "Nanoindentation investigation of creep properties of calcium silicate hydrates." *Cem. Concr. Res.*, 52(Oct), 38–52.

Voigt, W. (1890). "Ueber die innere Reibung fester Koeper, insbesondere der Krystalle [Concerning the inner friction of solids, in particular of crystals]." *Abhandlungen der Koeniglichen Gesellschaft der Wissenschaften in Goettingen*, 36, 3–43 (in German).

Youssef, M., Pellenq, R. J.-M., and Yildiz, B. (2011). "Glassy nature of water in an ultraconfining disordered material: The case of calcium-silicate-hydrate." *J. Am. Chem. Soc.*, 133(8), 2499–2510.